Supplementary materials

De novo phytosterol synthesis by an animal

Dolma Michellod[1], Tanja Bien[2], Daniel Birgel[3], Marlene Jensen[5], Manuel Kleiner[5], Sarah Fearn[4], Caroline Zeidler[1], Harald R Gruber-Vodicka[1], Nicole Dubilier[1,6*], Manuel Liebeke[1*]

[1] Max Planck Institute for Marine Microbiology, Celsiusstraße 1, 28359 Bremen, Germany

[2] Institute of Hygiene, University of Münster, Robert-Koch-Str. 41, 48149, Münster, Germany

[3] Institute for Geology, Center for Earth System Research and Sustainability, University of Hamburg, Bundesstraße 55, 20146 Hamburg, Germany

[4] Department of Materials, Imperial College London, London SW7 2AZ, United Kingdom

[5] Department of Plant and Microbial Biology, NC State University, Raleigh, NC 27695, United States

[6] MARUM, Center for Marine Environmental Sciences, University of Bremen, 28359 Bremen, Germany

*corresponding authors: mliebeke@mpi-bremen.de, ndubilier@mpi-bremen.de

Supplementary Information

Sitosterol is present in the environment of the gutless annelids in concentrations sufficient to sustain the growth of small sterol-auxotrophic invertebrates. Chemical analysis of pore water profiles collected in the vicinity of seagrass meadows, the habitat of many gutless annelids, revealed an irregular distribution of sterols. Some samples, such as those collected near *Posidonia oceanica* seagrass meadows off the island of Elba (Mediterranean), had cholesterol and sitosterol present in the nano- to micro-molar range **(Supplementary Figure 3).** Samples collected in Belize (Caribbean), in the vicinity of the seagrasses *Thalassia testudinum* and *Syringodium filiforme,* were devoid of detectable amounts of sitosterol or cholesterol. Seagrasses, like terrestrial plants, exude organic compounds into the substrate surrounding their roots, the rhizosphere (Sogin et al., 2021; Vives-Peris et al., 2020). The sterol profile of *P. oceanica* roots was composed of sitosterol (69%), stigmasterol (11%) and campesterol (20%). *P. oceanica* could thus be the origin of the sitosterol in the porewater, but cannot be the source of cholesterol as it was not present in its tissues. Cholesterol and sitosterol concentrations measured in the porewater environment (ranging from 25 nM to 3 µM) are in the range of reported minimal dietary sterol requirements for small sterol-auxotrophic invertebrates (Carvalho et al., 2010; Lu et al., 1977). Furthermore, the sterols in the porewater could pass through the cuticle of the worm as it is permeable to substances up to 70 kDa (Dubilier et al., 2006).

The isotopic signature of the sterols in the worms exclude an environmental origin. Results from GC-IRMS with single metabolite resolution showed that the sitosterol present in seagrass tissue had $\delta^{13}C$ values ranging from −21 ‰ to −15 ‰ (**Figure 1E**). These values are in accordance with bulk measures of isotopic composition for *P. oceanica* which range from −16.4 ‰ to −8.3 ‰ (Cooper & DeNiro, 1989; Jennings et al., 1997; Lepoint et al., 2004; McMillan et al., 1980; Pinnegar & Polunin, 2000; Vizzini et al., 2010), and also match values previously reported for sterols in other seagrasses (Canuel et al., 1997). Sterols from sediment porewater had $\delta^{13}C$ values of −30 ‰ to −26 ‰ (**Figure 1E**), which are similar to previously reported ranges (Canuel et al., 1997; Dauby, 1989; Fry et al., 1983; Thayer et al., 1978) and

about 10 ‰ lower than the sterols from *P. oceanica*. This difference reflects the mixed sources of the sterols present in the sediment, most of which are likely planktonic in origin.

The total sterol content of gutless annelids is comparable to the content of other worms. Measurements of metabolites in single *Olavius algarvensis* worms with mass spectrometry revealed a total free sterol content of 3.44 ± 0.04 µg (*n* = 12). Assuming an average wet weight per worm of 1 mg, sterols represent 0.34 % wet weight, a value similar to reported percentages for terrestrial and aquatic worms (Ballantine et al., 1978; McLaughlin, 1971a; Voogt, 1973a; Wilber & Bayors, 1947).

SMTs in rotifers. The rotifer sequences grouped together to form a sister group to unicellular eukaryotes SMT (**Figure 3**). The rotifers were isolated from different environments and had access to different food resources, which suggests that the recovered sequences were not a result of contamination. Sterol auxotrophy has been proposed for rotifers (Wacker & Martin-Creuzburg, 2012) and C_{24}-SMTs might play a different role in these organisms. Animal sterol auxotrophs usually lack the three enzymes responsible for the transformation of squalene into lanosterol: farnesyl-diphosphate farnesyltransferase 1 (FDFT1), squalene monooxygenase (SQE) and lanosterol synthase (LAS) (Shamsuzzama et al., 2020). However, the presence of downstream cholesterol synthesis genes has been reported in sterol auxotrophs. Some of these sterol enzymes retain their catalytic functions and are involved in the conversion of dietary sterols into cholesterol (Meyer et al., 1979; Shamsuzzama et al., 2020), while others now have distinct functions (Oh et al., 2017; Shamsuzzama et al., 2020). The function performed by C_{24}-SMT enzymes in rotifers would benefit from further study.

Supplementary Figures and Tables

List of Supplementary Figures

List of Supplementary Tables

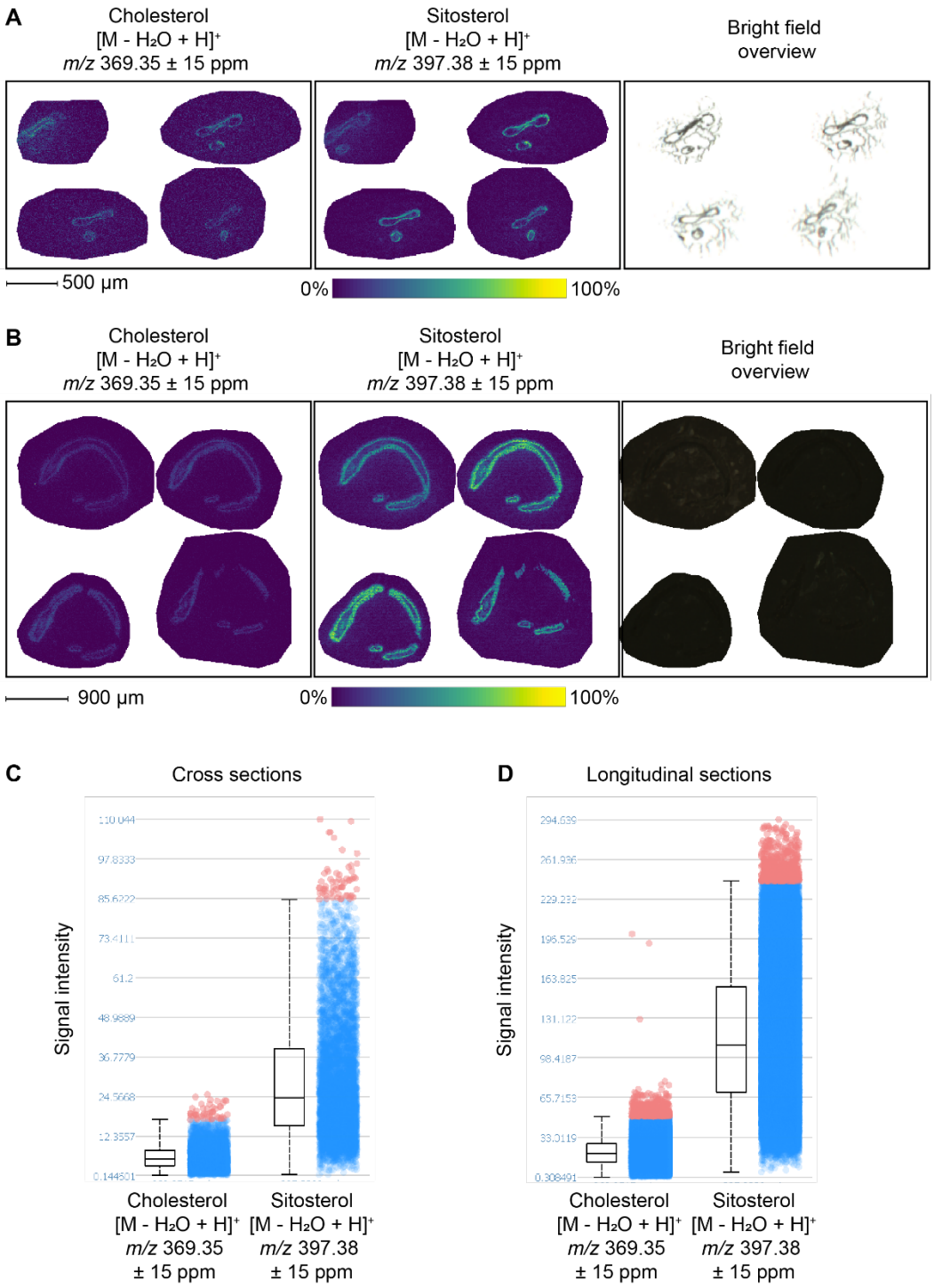

Supplementary Figure 1 | Sitosterol and cholesterol are evenly distributed throughout *Olavius algarvensis* tissues. Panels show cholesterol ([M-H2O+H]$^+$ at *m/z* 369.352) and sitosterol ([M-H2O+H]$^+$ at *m/z* 397.382) distribution in *O. algarvensis* cross sections (**A**) and longitudinal sections (**B**) measured by MALDI-2-MSI. Sitosterol is more abundant than cholesterol in the worm tissues (**C** and **D**).

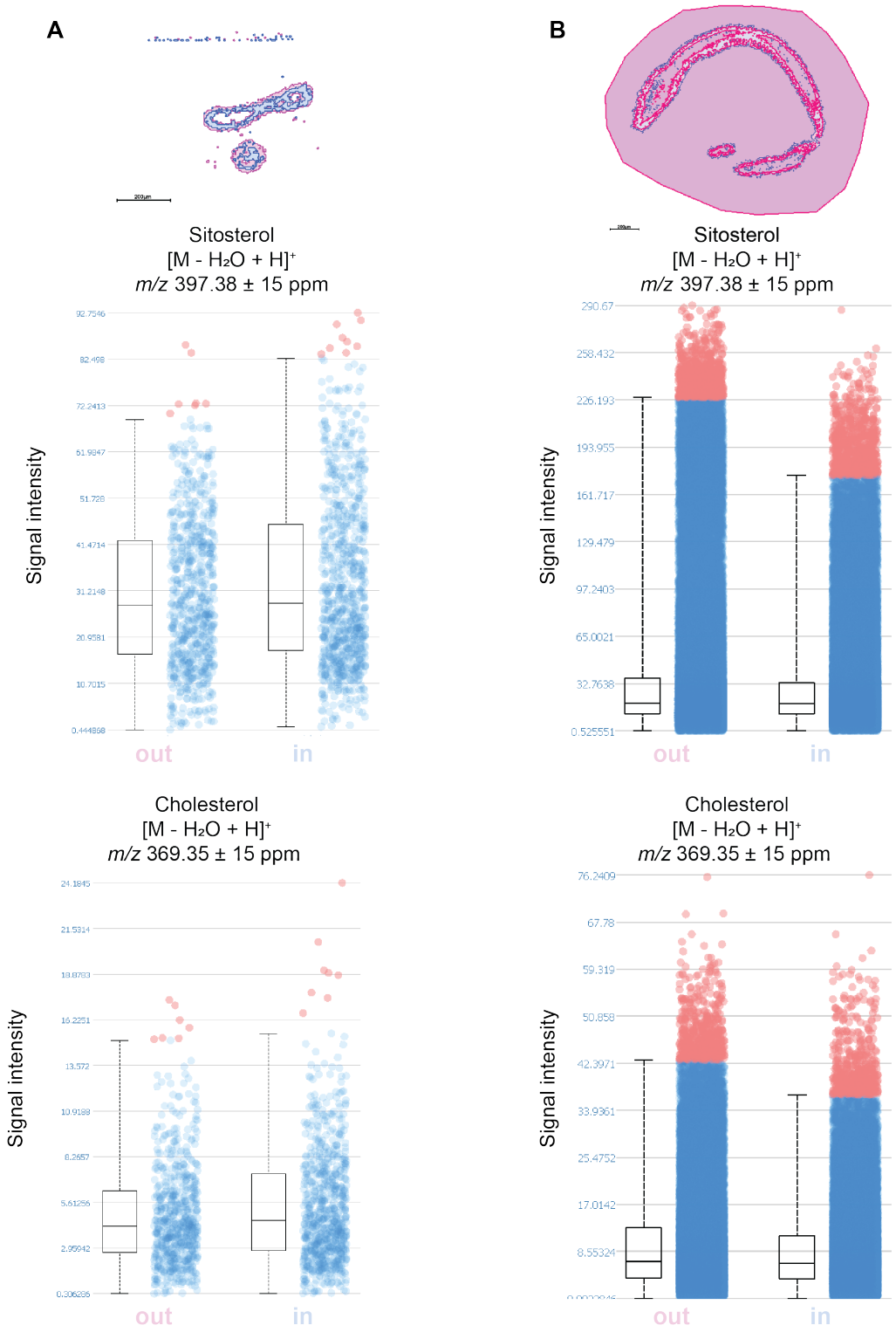

Supplementary Figure 2 | No tissue-specific distribution of cholesterol and sitosterol in *Olavius algarvensis*. Both sterols were uniformly distributed throughout the animals' tissues. Distribution of cholesterol and sitosterol as measured with MALDI-2-MSI. The data was segmented and the signal intensity of both sterols measured to investigate tissue specific sterol distribution in cross sections (**A**) and longitudinal sections (**B**). The colonized tissues (out) do not contain more sterols than the host-only tissues (in). The presence of the symbionts does not influence the sterol distribution in the host tissues.

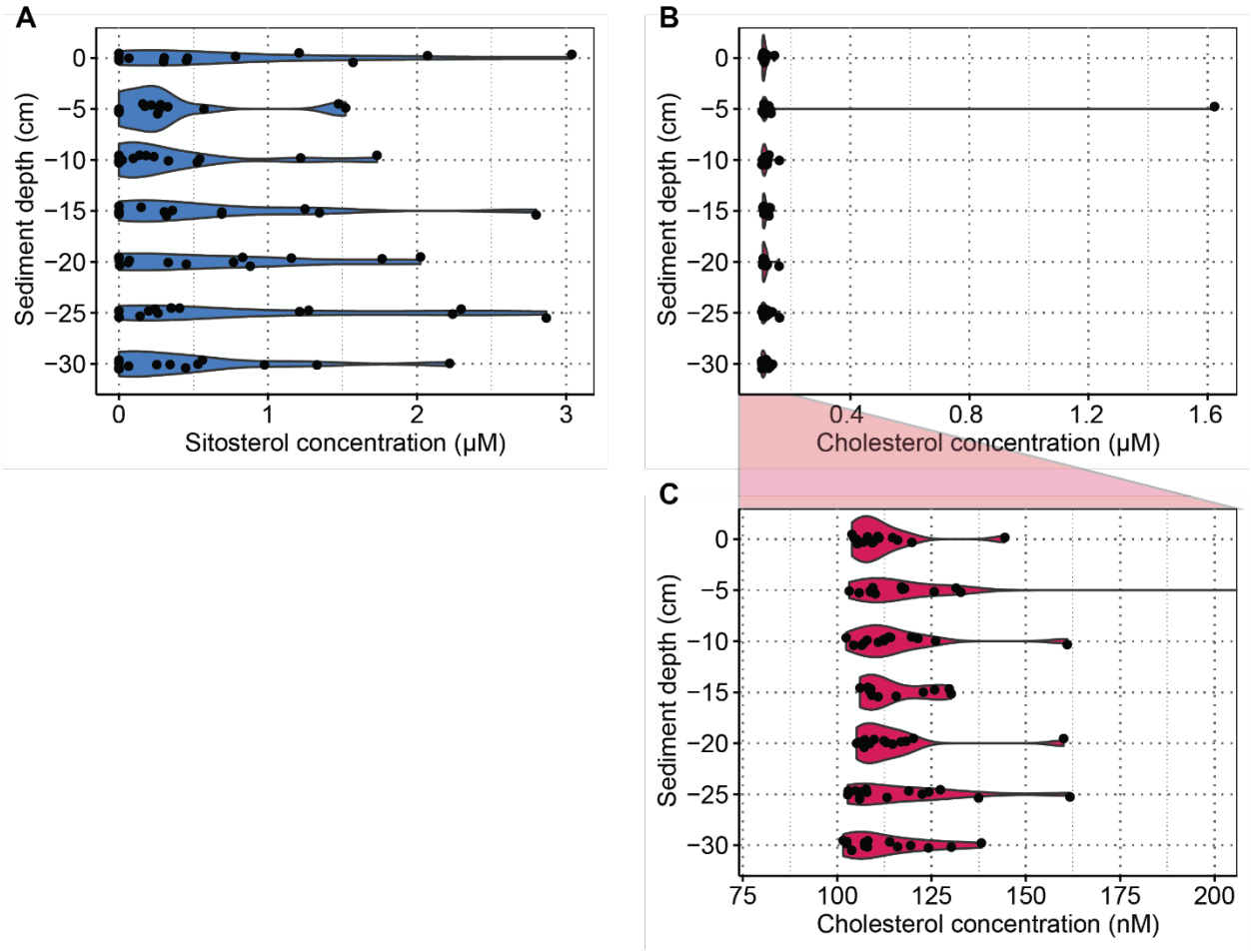

Supplementary Figure 3 | Sediment porewater below a *P. oceanica* meadow (Elba, Italy) contained sitosterol and cholesterol. A, Sitosterol (blue) was present at micromolar concentration under the seagrass bed. **B,** Cholesterol (red) was present in nanomolar concentrations under the seagrass bed, with one exception in the low micromolar range. **C,** Magnified view of **B** to show the variation in cholesterol concentrations between 100 to 200 nanomolar.

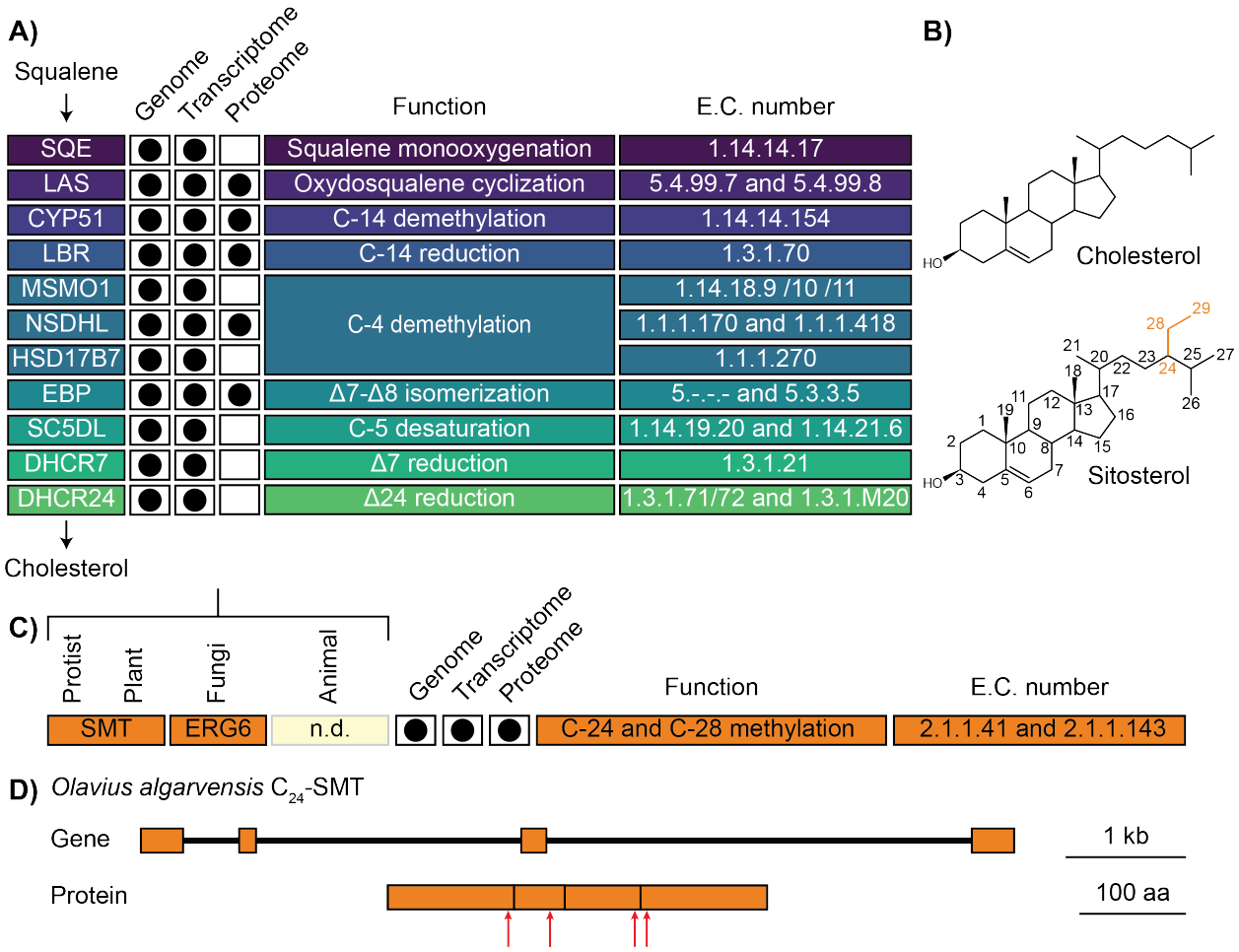

Supplementary Figure 4 | *Olavius algarvensis* encodes and expresses all the enzymes needed to synthesize sitosterol from an intermediate of the cholesterol synthesis pathway. **A,** All 11 enzymes involved in cholesterol synthesis were encoded and expressed by *O. algarvensis*. **B,** An ethyl group attached to the sterol side chain differentiates the phytosterol sitosterol from the animal sterol cholesterol. **C,** *O. algarvensis* encodes and expresses a homolog of C_{24}-SMT, an enzyme not previously found in bilaterial animals and essential to sitosterol synthesis. Dots indicate detection in the genome, transcriptome and proteome of *O. algarvensis*. **D,** The *O. algarvensis* C_{24}-SMT gene consists of 4 exons forming a 1071 bp open reading frame encoding a 356 amino-acid polypeptide. The four conserved regions of the enzyme are highlighted by red arrows.

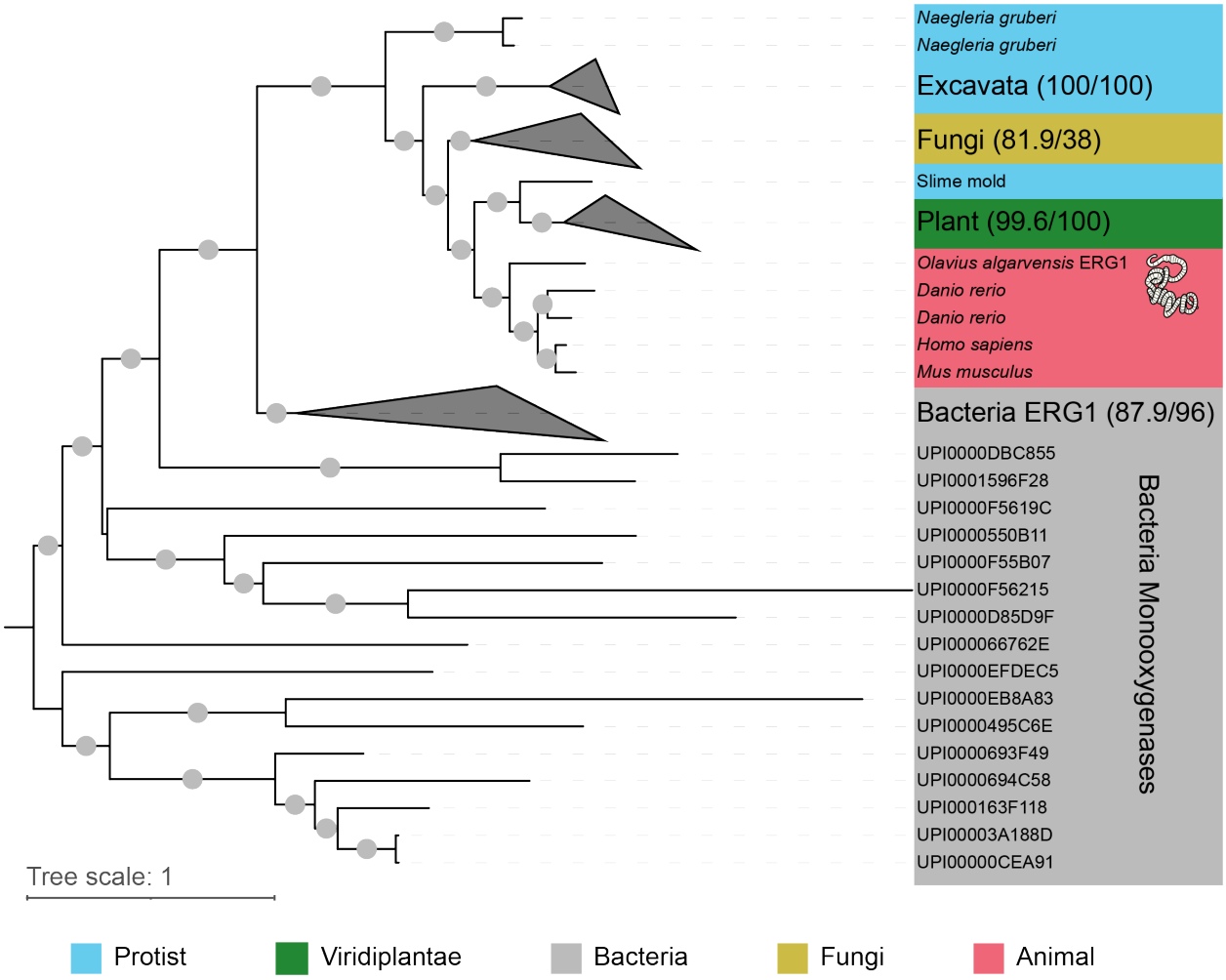

Supplementary Figure 5 | *Olavius algarvensis* squalene monooxygenase (ERG1) sequence clusters with animal sequences. Maximum likelihood tree of ERG1 amino acid sequences. Bootstrap values ≥90% are shown with a grey circle. The bootstrap value and branch support value are indicated in brackets for collapsed groups. The tree was rooted at midpoint in iTOL.

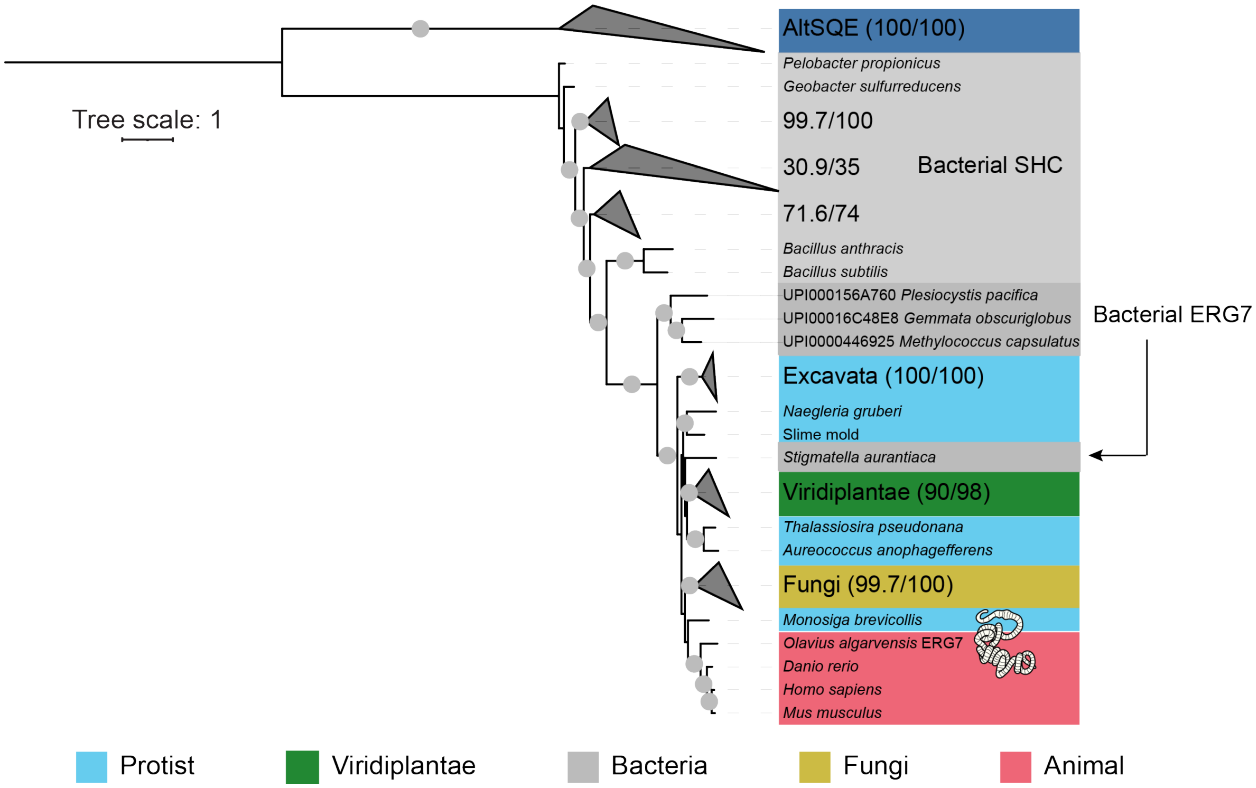

Supplementary Figure 6 | *Olavius algarvensis* lanosterol synthase (ERG7) sequence clusters with animal sequences. Maximum likelihood tree of ERG7 amino acid sequences, alternative squalene epoxidase (AltSQE) and the bacterial squalene-hopene cyclase (SHC) were used as outgroups. Bootstrap values ≥90% are shown with a grey circle. The bootstrap value and branch support value are indicated in brackets for collapsed groups. The tree was rooted at midpoint in iTOL.

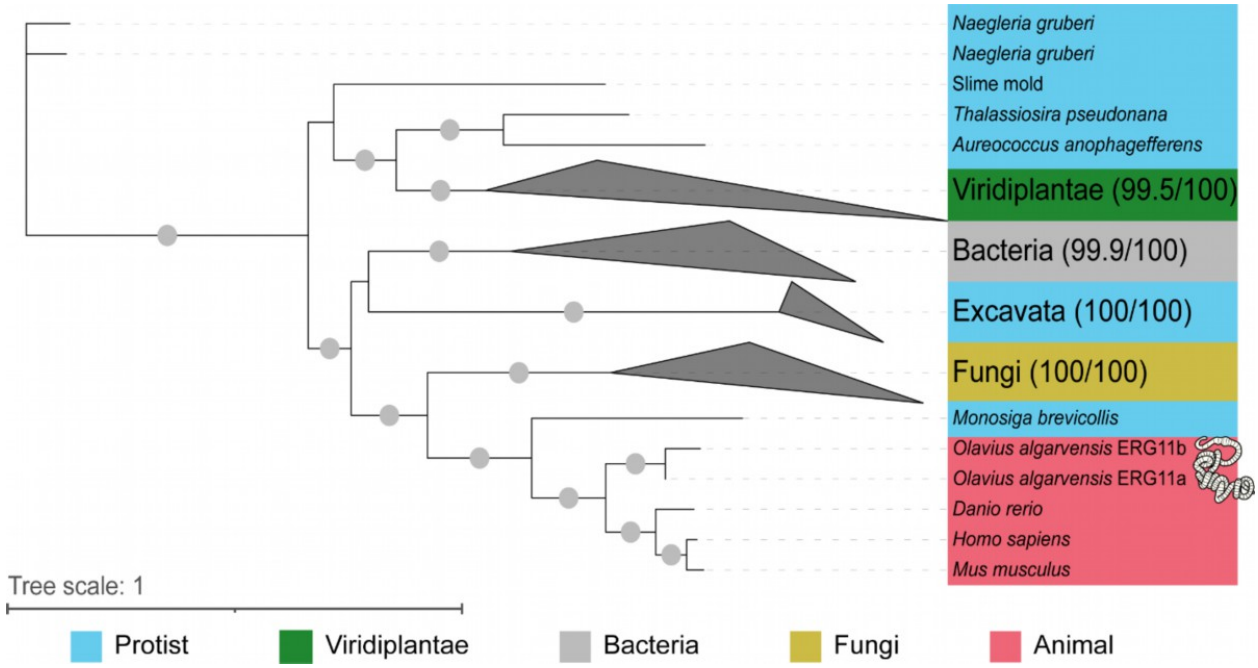

Supplementary Figure 7 | *Olavius algarvensis* sterol delta-14-demethylase (ERG11) sequences cluster with animal sequences. Maximum likelihood tree of ERG11 amino acid sequences. Bootstrap values ≥90% are marked with a grey circle. The bootstrap value and branch support value are indicated in brackets for collapsed groups. The tree was rooted at midpoint in iTOL.

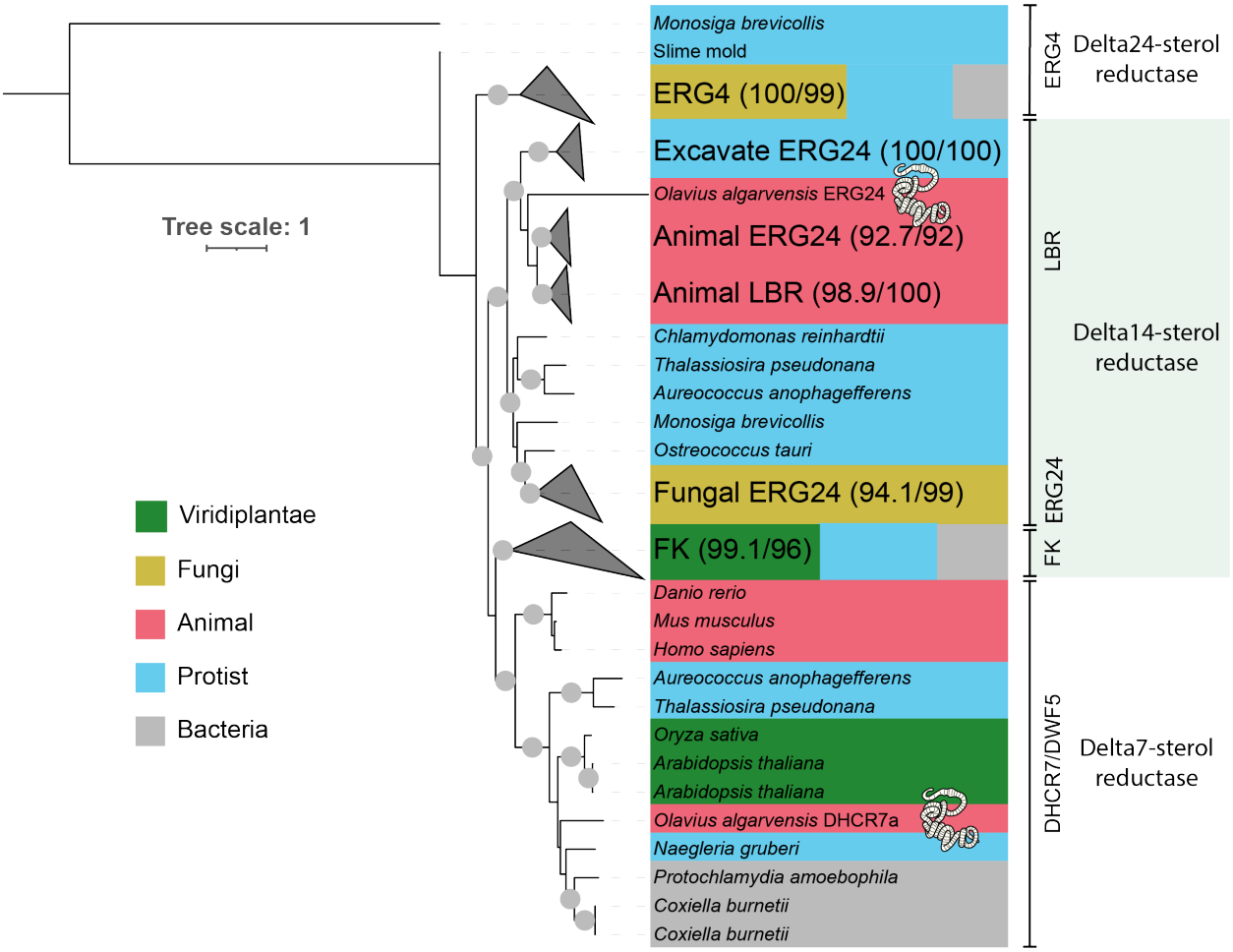

Supplementary Figure 8 | *Olavius algarvensis* delta14-sterol reductase (ERG24) sequence clusters with animal sequences while the sterol 7-dehydrocholesterol reductase (DHCR7) cluster with plants and unicellular sequences. The placement of *O. algarvensis* DHCR7 might indicate affinity for a substrate different from that of other animals. Maximum likelihood tree of the (ERG4)-(DHCR7/DWF5)-(ERG24/LBR/FK) protein family, here we have an example of enzyme performing different steps in fungi, animals and plant but that are evolutionary related. Bootstrap values ≥90% are marked with a grey circle. The bootstrap value and branch support value are indicated in brackets for collapsed groups. The tree was rooted at midpoint in iTOL.

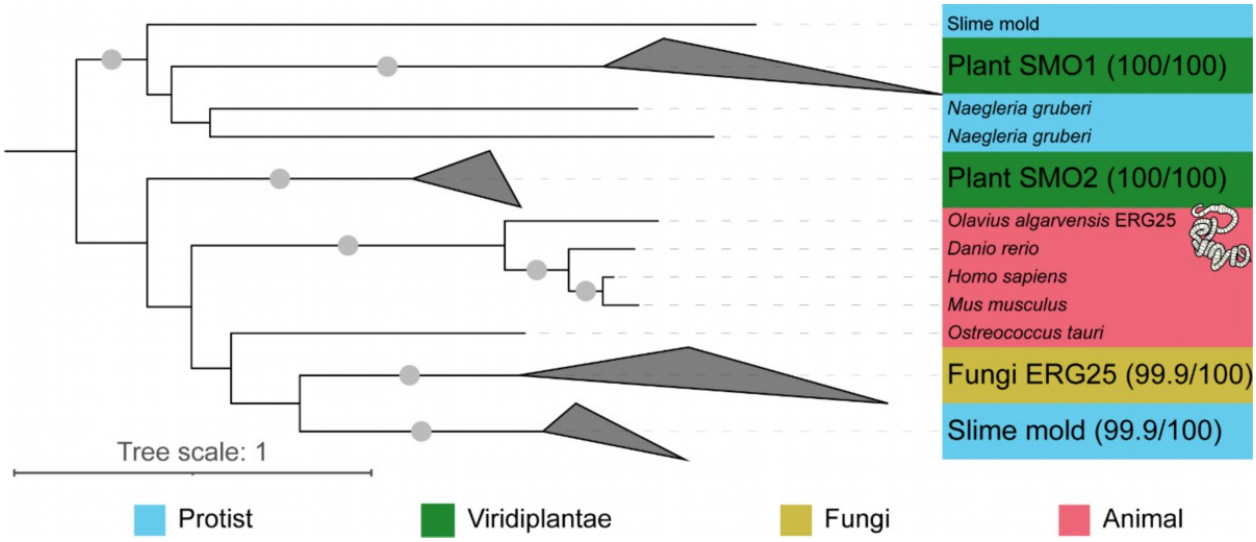

Supplementary Figure 9 | *Olavius algarvensis* methylsterol monooxygenase sequence clusters with animal sequences. Maximum likelihood tree of methylsterol monooxygenase (SMO1/SMO2-ERG25-MSMO) amino acid sequences. Bootstrap values ≥90% are marked with a grey circle. The bootstrap value and branch support value are indicated in brackets for collapsed groups. The tree was rooted at midpoint in iTOL.

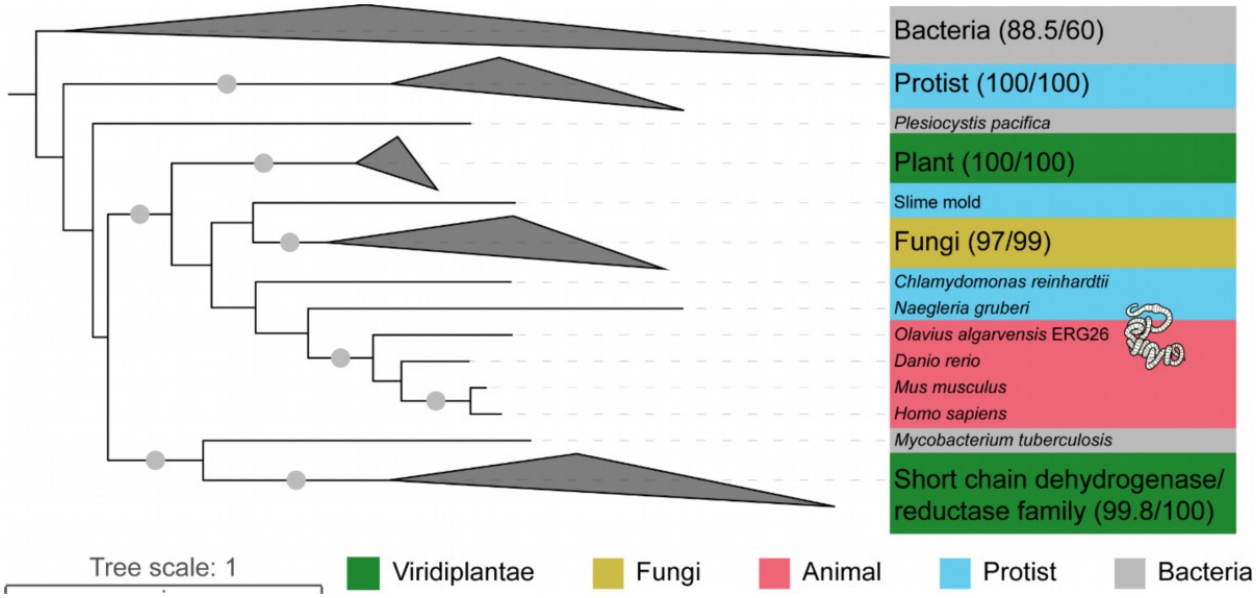

Supplementary Figure 10 | *Olavius algarvensis* sterol-4-alpha-carboxylate 3-dehydrogenase, decarboxylating sequence clusters with animal sequences. Maximum likelihood tree of sterol-4-alpha-carboxylate 3-dehydrogenase (HSD-NSDHL-ERG26) amino acid sequences. Bootstrap values ≥90% are marked with a grey circle. The bootstrap value and branch support value are indicated in brackets for collapsed groups. The tree was rooted at midpoint in iTOL.

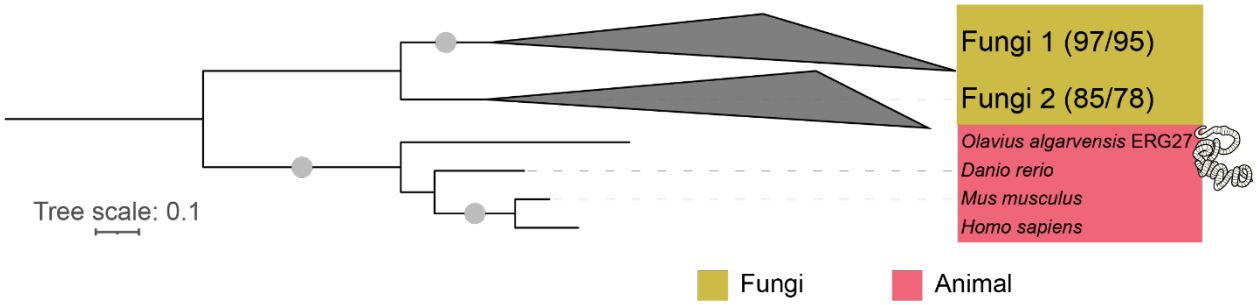

Supplementary Figure 11 | *Olavius algarvensis* 3-keto reductase (ERG27) sequence clusters with animal sequences. Maximum likelihood tree of ERG27 amino acid sequences. Bootstrap values ≥90% are marked with a grey circle. The bootstrap value and branch support value are indicated in brackets for collapsed groups. The tree was rooted at midpoint in iTOL. The gene performing C-3 keto reduction in plants and protists is still unknown.

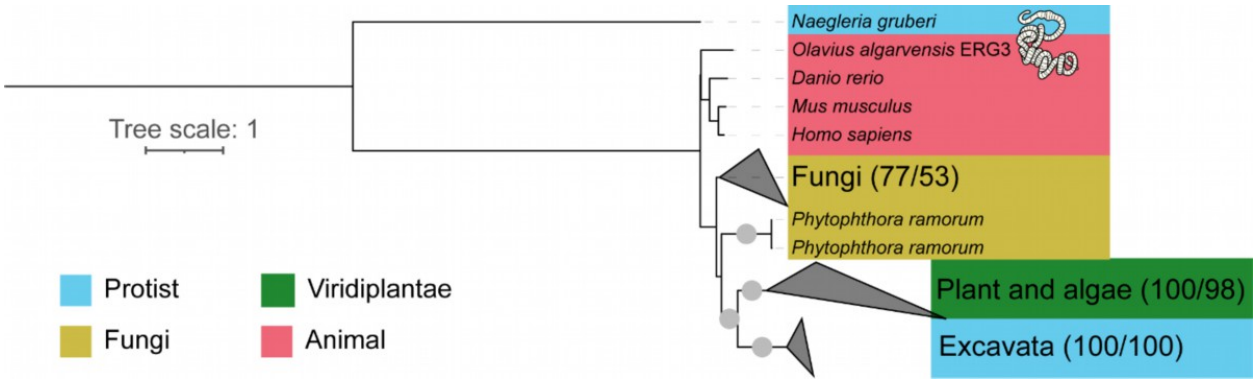

Supplementary Figure 12 | *Olavius algarvensis* sterol C-5 desaturase (ERG3) sequence clusters with animal sequences. Maximum likelihood tree of ERG3 amino acid sequences. Bootstrap values ≥90% are marked with a grey circle. The bootstrap value and branch support value are indicated in brackets for collapsed groups. The tree was rooted at midpoint in iTOL.

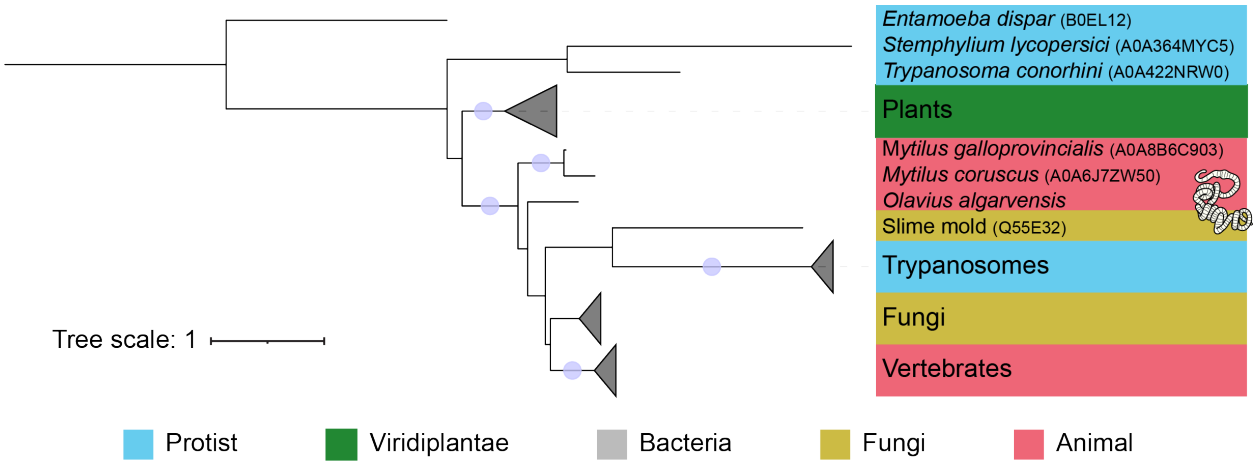

Supplementary Figure 13 | *Olavius algarvensis* detla7-delta8-sterol isomerase (EBP) sequence clusters with animal and fungal sequences. Maximum likelihood tree of EBP amino acid sequences. Bootstrap values ≥95% are marked with a grey circle. The tree was rooted at midpoint in iTOL.

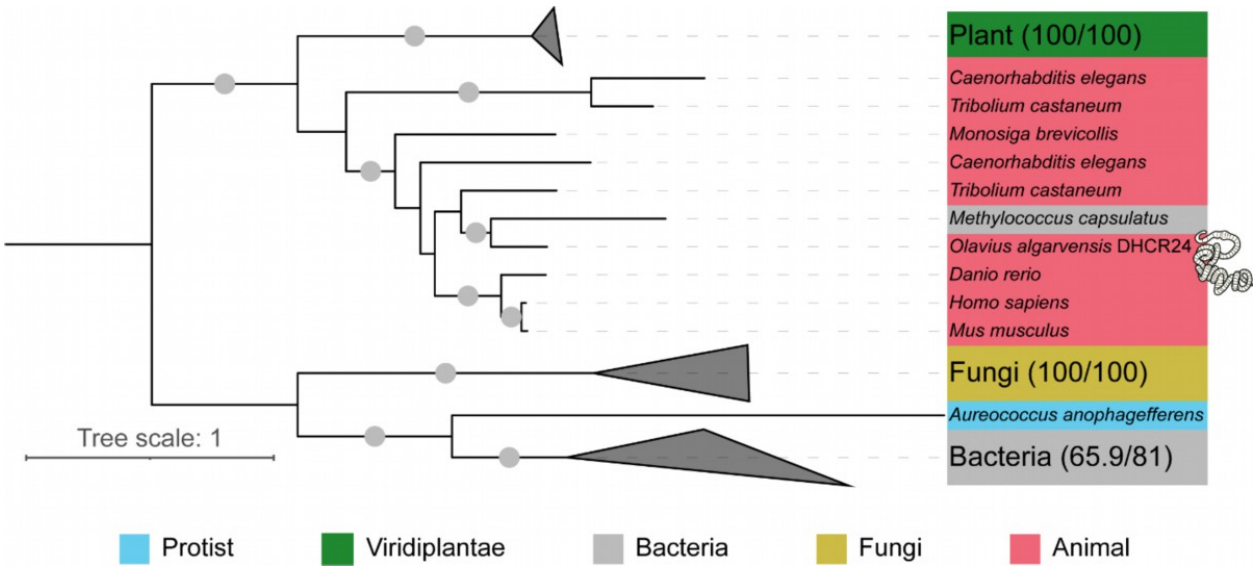

Supplementary Figure 14 | *Olavius algarvensis* sterol 24-dehydrocholesterol reductase (DHCR24) sequence clusters with animal sequences. Maximum likelihood tree of DHCR24 amino acid sequences. Bootstrap values ≥90% are marked with a grey circle. The bootstrap value and branch support value are indicated in brackets for collapsed groups. The tree was rooted at midpoint in iTOL.

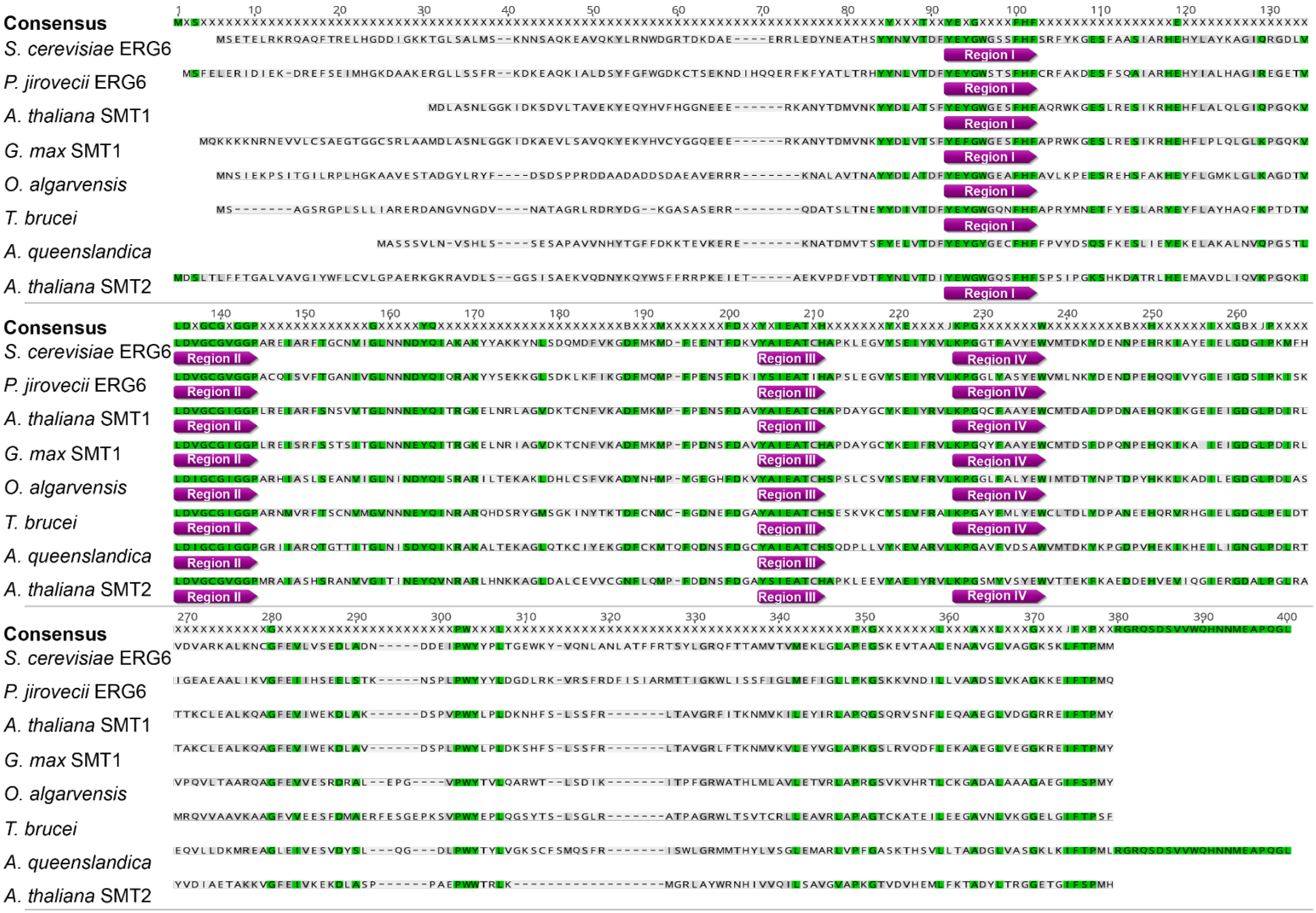

Supplementary Figure 15 | Alignment of C-24 sterol methyltransferase (C_{24}-SMT) amino acid sequences. Sequences from: fungi, *Saccharomyces cerevisiae* (P25087) and *Pneumocystis* (Q96WX4); plants: *Arabidopsis thaliana* SMT1 (Q9LM02) and SMT2 (Q39227) and *Glycine max* SMT1 (Q43445); gutless annelid: *Olavius algarvensis* (this study); excavate: *Trypanosoma brucei* (Q4FKJ2); and sponge: *Amphimedon queenslandica* (A0A1X7ULF8). The sequences were aligned using ClustalW (Geneious). Purple labels indicate sterol (II) and AdoMet (I, III and IV) binding regions.

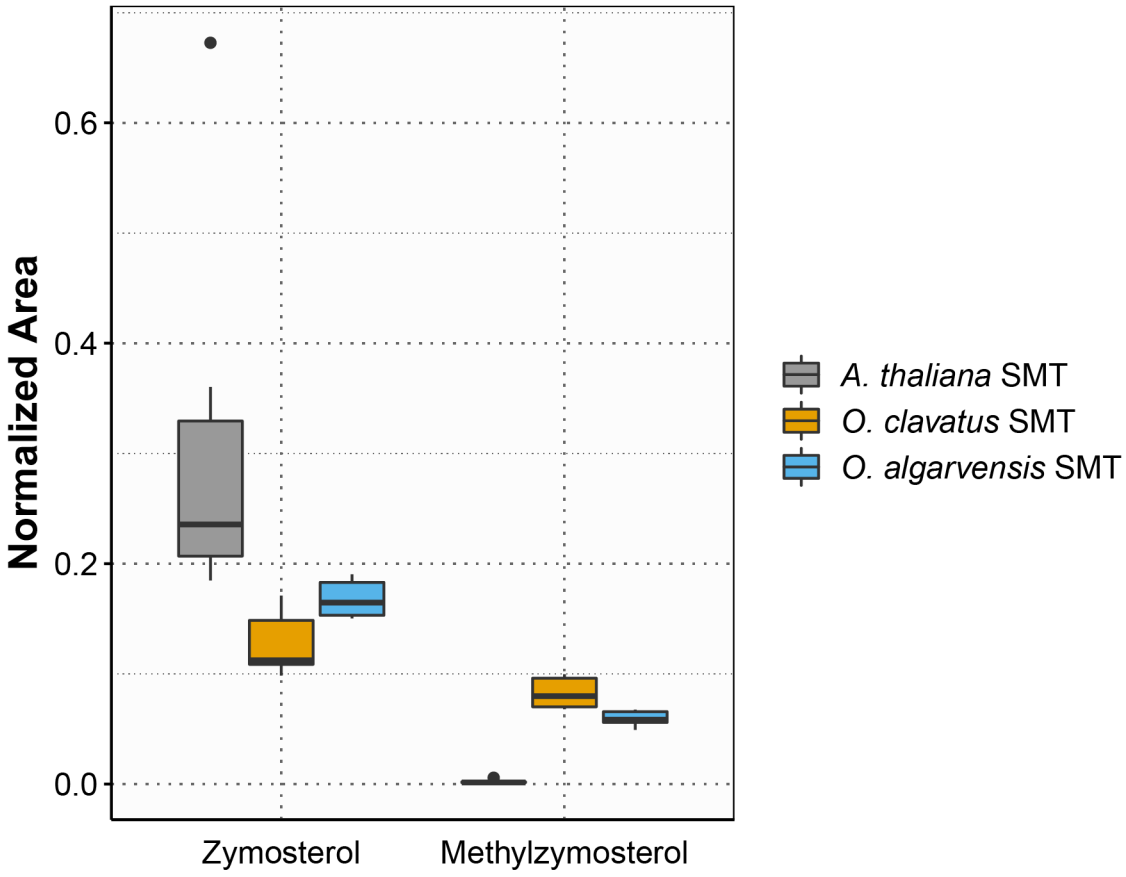

Supplementary Figure 16 | The C_{24}-SMT of *Olavius* spp. used zymosterol as a substrate for the first methylation. . *Arabidopsis thaliana* C_{24}-SMT did not methylate zymosterol. The heterologously expressed C_{24}-SMT enzymes from both *O. algarvensis* and *O. clavatus* were able to methylate zymosterol to methylzymosterol. The peak of the substrate (zymosterol) and of the product (methylzymosterol) were integrated at the end of the enzymatic assay, in which *E. coli* expressed C_{24}-SMT from each taxon (n = 5 in each case) was incubated with zymosterol as substrate. The abundance was normalized with an internal standard.

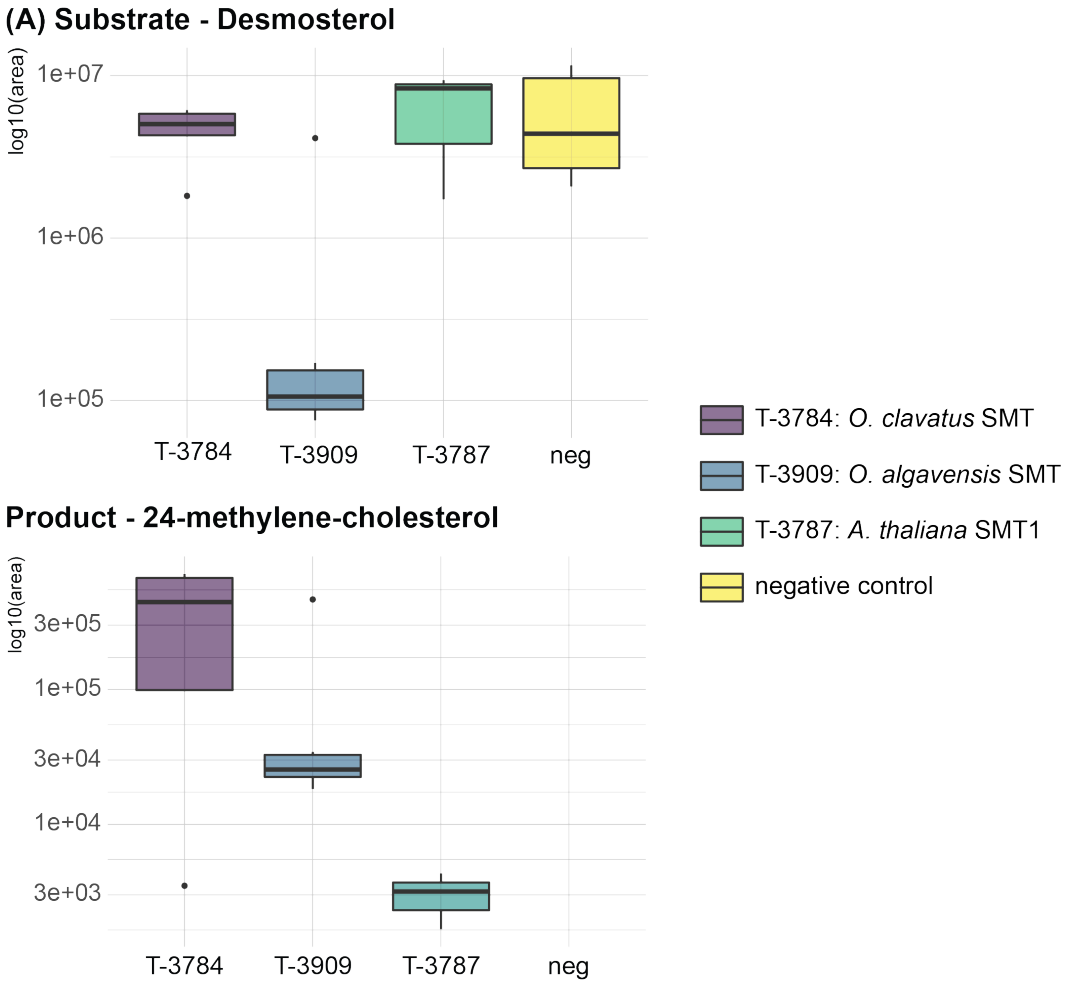

Supplementary Figure 17 | The C_{24}-SMT of *Olavius* spp. used desmosterol as a substrate for the first methylation step. *Arabidopsis thaliana* C_{24}-SMT was not able to methylate desmosterol. The heterologously expressed C_{24}-SMT enzymes from both *O. algarvensis* and *O. clavatus* were able to methylate desmosterol to produce 24-methylene-cholesterol. The abundance of the substrate (desmosterol) and the product (24-methylene-cholesterol) were measured at the end of the enzymatic assay, in which *E. coli* expressed C_{24}-SMT from each taxon (n = 5 in each case) was incubated with desmosterol as substrate.

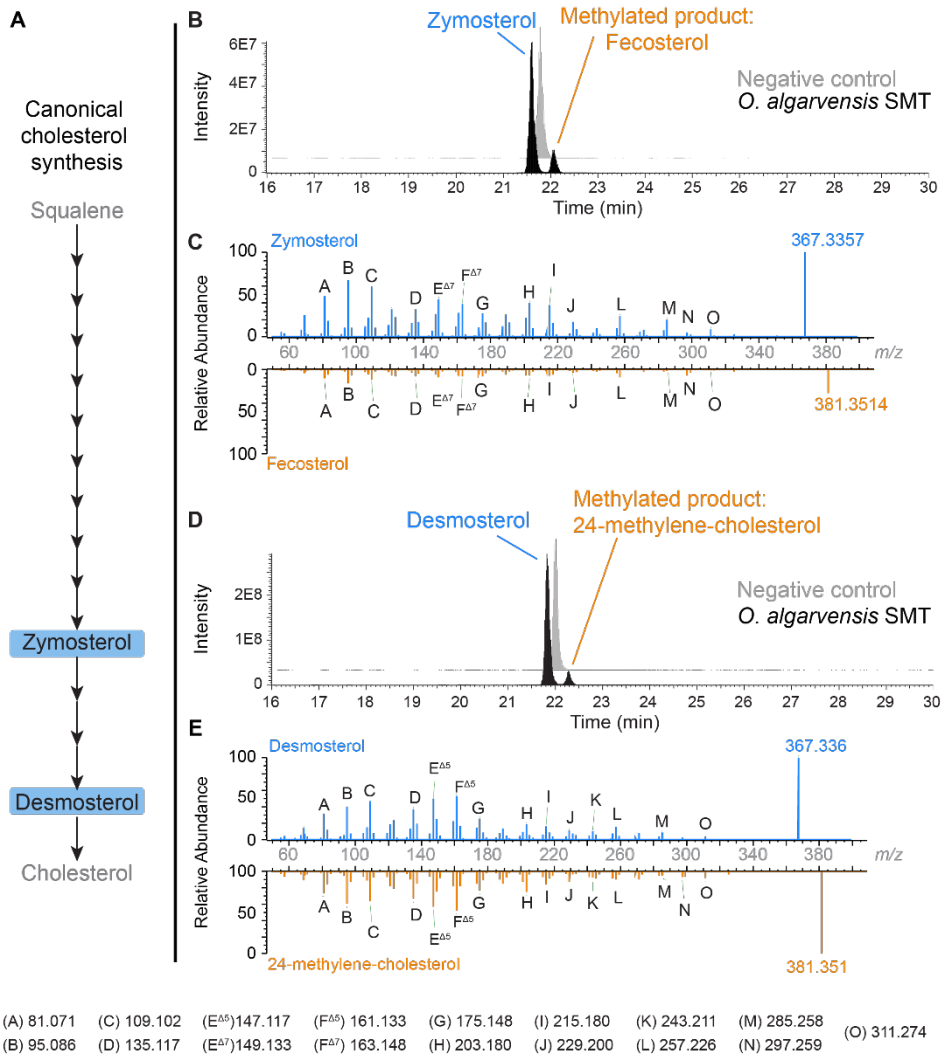

Supplementary Figure 18 | C_{24}-SMT of *Olavius algarvensis* uses two intermediates of the cholesterol synthesis, zymosterol and desmosterol, as substrates for methylation. A, Zymosterol and desmosterol are intermediates of the classical animal cholesterol synthesis. They are produced in the second half of the cholesterol synthesis pathway. **B and D,** *O. algarvensis* C_{24}-SMT, after overexpression in *E. coli*, added a methyl group to the side chain of zymosterol and desmosterol. LC-MS chromatograms of the enzymatic assay performed with zymosterol and desmosterol as substrates**. C and E,** The substrates and methylated products were identified by MS/MS.

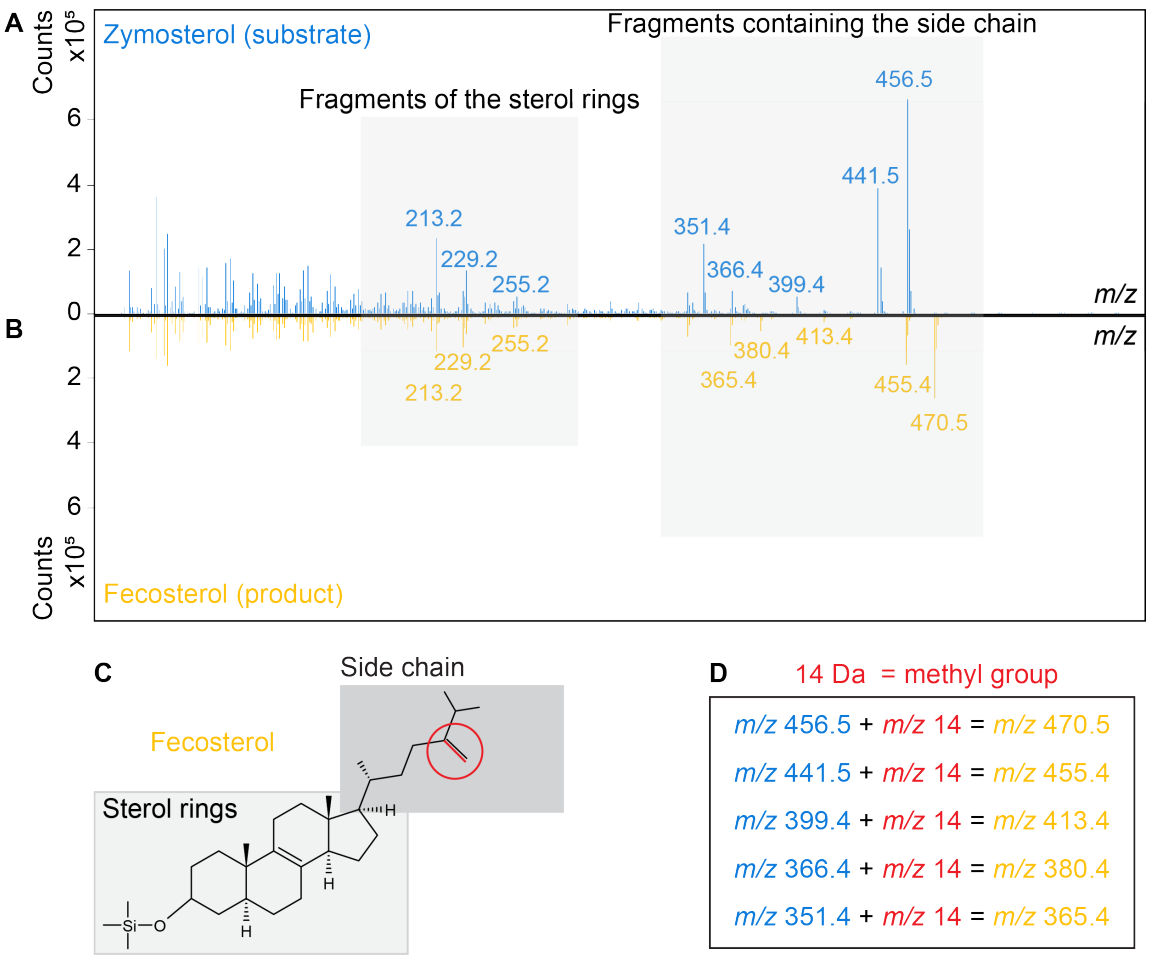

Supplementary Figure 19 | The C_{24}-SMT of *Olavius algarvensis* added a methyl group to the side chain of zymosterol. A, B, Representative mass spectra of zymosterol **(A)** and the compound identified as fecosterol (24-methylene-zymosterol) **(B). C,** Structure of fecosterol, with the methyl group highlighted in red. **D,** In the comparison of the mass spectra of zymosterol and fecosterol, the fragments containing the side chain were shifted by 14 Da, a difference that represents the addition of a methyl group. No mass shift was observed in the sterol ring fragments. These results indicate that a methyl group was added to the zymosterol side chain.

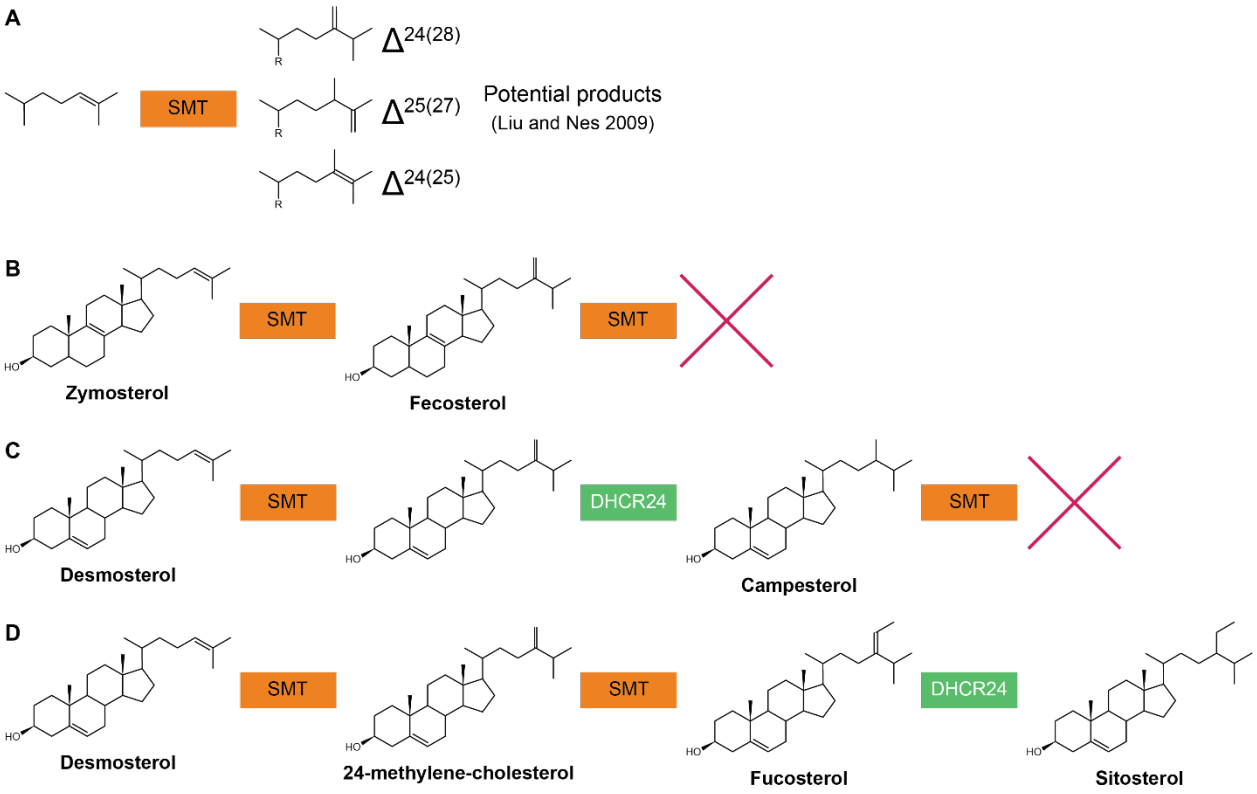

Supplementary Figure 20 | Potential substrates for the second C_1-transfer based on the results of the first C_1-transfer. A, C_{24}-SMT can produce different products. *O. algarvensis* C_{24}-SMT mainly produced methylene ($\Delta^{24(28)}$) products. **B,** *O. algarvensis* C_{24}-SMT methylates zymosterol to produce fecosterol. Fecosterol was not methylated further by *O. algarvensis* C_{24}-SMT. **C and D,** *O. algarvensis* C_{24}-SMT added a methyl group to demosterol to produce 24-methylene-cholesterol. **C,** The methylene group is then likely reduced by sterol C24-reductase (DHCR24), producing campesterol. Campesterol was identified as a potential candidate for the second methylation step but *O. algarvensis* C_{24}-SMT could not use it as a substrate. **D,** The product of desmosterol methylation could also be used directly as a substrate for the second methylation. *O. algarvensis* C_{24}-SMT added a methyl group to 24-methylene-cholesterol, producing fucosterol. DHCR24, which is expressed based on its presence in *O. algarvensis* transcriptomes, could then remove the $\Delta^{24(28)}$ double bond and transform fucosterol into sitosterol.

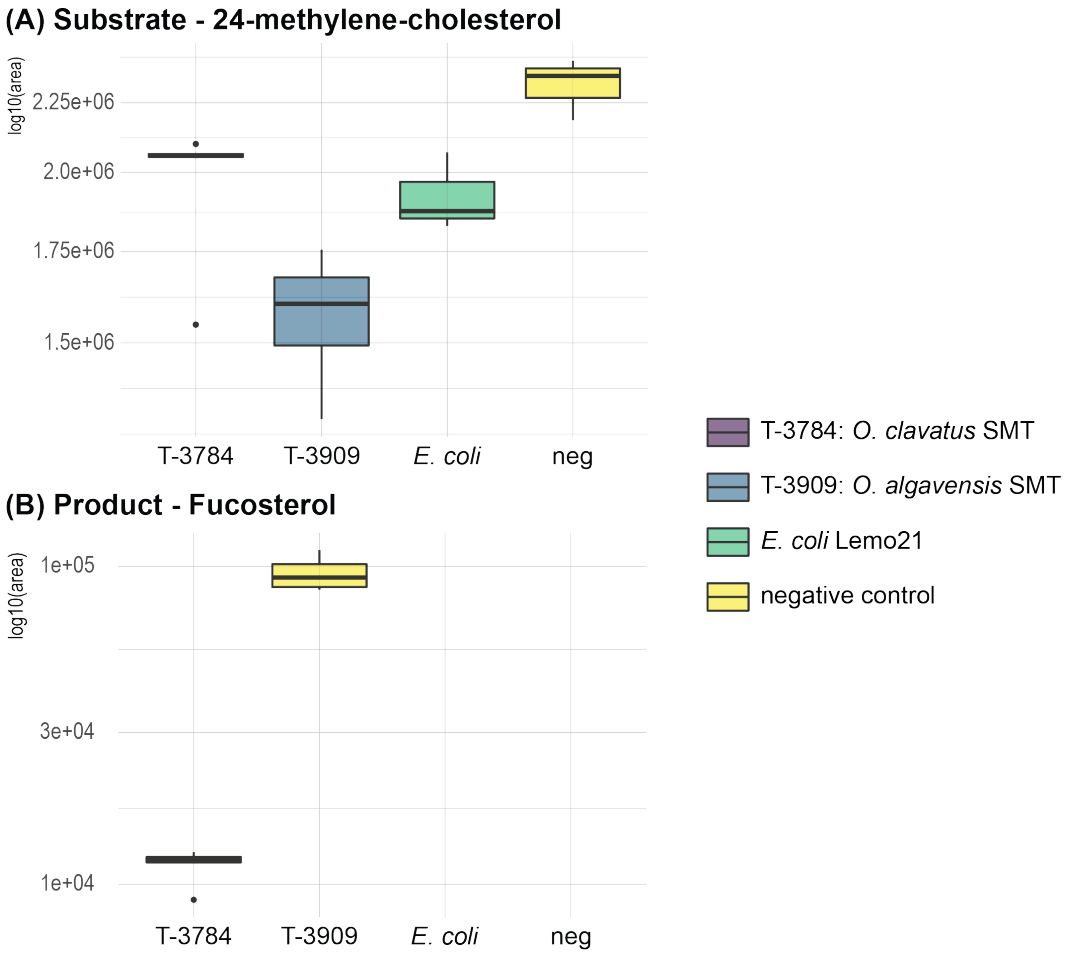

Supplementary Figure 21 | The C_{24}-SMT of *Olavius* spp. use 24-methylene-cholesterol as a substrate for the second methylation reaction. The enzymes from both *O. algarvensis* and *O. clavatus* used 24-methylene-cholesterol as substrate and produced fucosterol. The abundance of the substrate (24-methylene-cholesterol) and the product (fucosterol) were integrated at the endpoint of the enzymatic assay, in which *E. coli* expressed C_{24}-SMT from each taxon (n = 5 in each case) was incubated with 24-methylene-cholesterol as substrate.

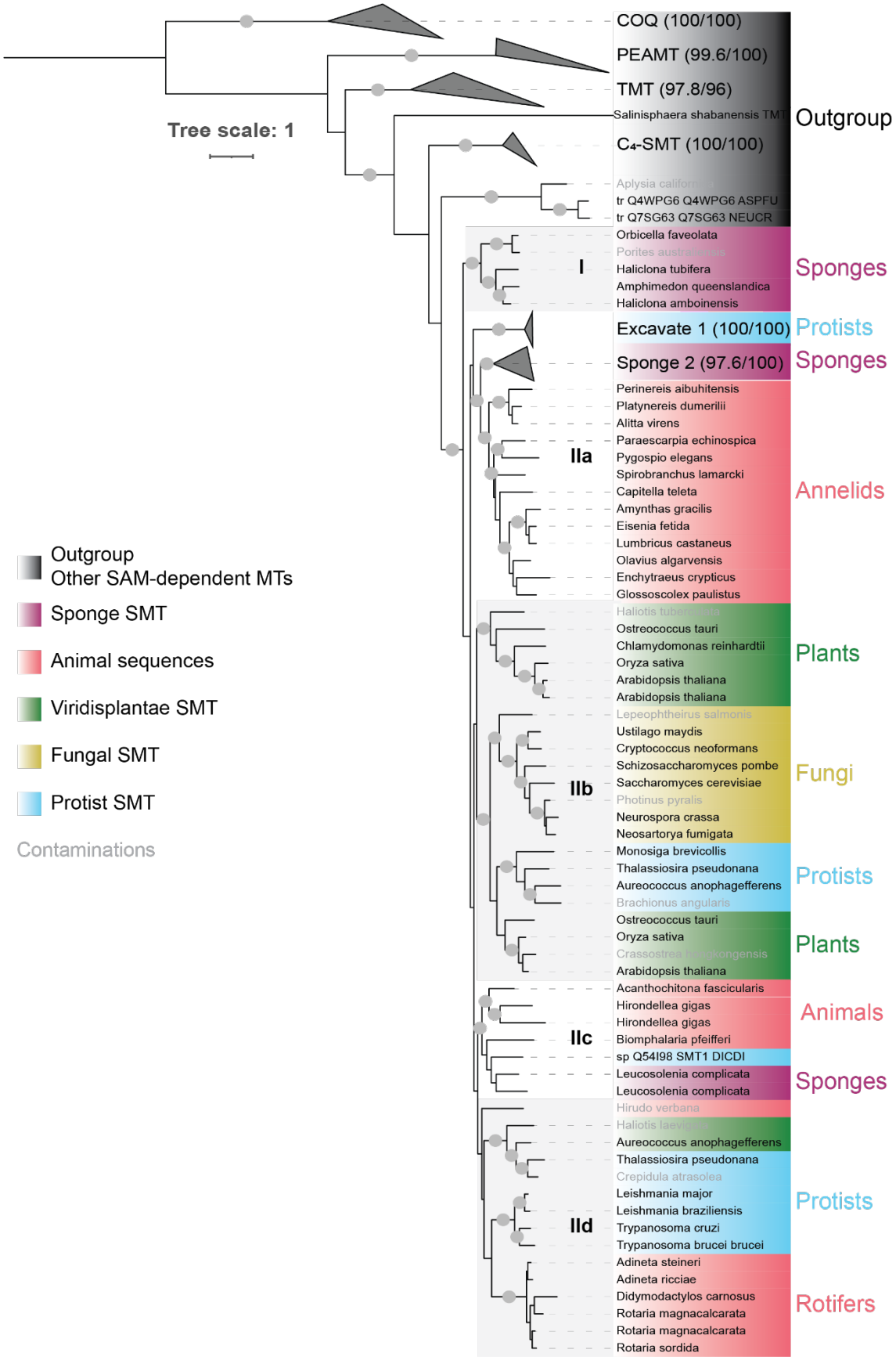
Tree scale: 1
COQ (100/100)
PEAMT (99.6/100)
TMT (97.8/96)
Salinisphaera shabanensis TMT
C4-SMT (100/100)
Aplysia californica
tr Q4WPG6 Q4WPG6 ASPFU
tr Q7SG63 Q7SG63 NEUCR
Outgroup
Orbicella faveolata
Porites australiensis
Haliclona tubifera
Amphimedon queenslandica
Haliclona amboinensis
I
Sponges
Excavate 1 (100/100)
Protists
Sponge 2 (97.6/100)
Sponges
Perinereis aibuhitensis
Platynereis dumerilii
Alitta virens
Paraescarpia echinospica
Pygospio elegans
Spirobranchus lamarcki
Capitella teleta
Amynthas gracilis
Eisenia fetida
Lumbricus castaneus
Olavius algarvensis
Enchytraeus crypticus
Glossoscolex paulistus
IIa
Annelids
Haliotis tuberculata
Ostreococcus tauri
Chlamydomonas reinhardtii
Oryza sativa
Arabidopsis thaliana
Arabidopsis thaliana
Plants
Lepeophtheirus salmonis
Ustilago maydis
Cryptococcus neoformans
Schizosaccharomyces pombe
Saccharomyces cerevisiae
Photinus pyralis
Neurospora crassa
Neosartorya fumigata
IIb
Fungi
Monosiga brevicollis
Thalassiosira pseudonana
Aureococcus anophagefferens
Protists
Brachionus angularis
Ostreococcus tauri
Oryza sativa
Crassostrea hongkongensis
Arabidopsis thaliana
Plants
Acanthochitona fascicularis
Hirondellea gigas
Hirondellea gigas
Biomphalaria pfeifferi
IIc
Animals
sp Q54I98 SMT1 DICDI
Leucosolenia complicata
Leucosolenia complicata
Sponges
Hirudo verbana
Haliotis laevigata
Aureococcus anophagefferens
Thalassiosira pseudonana
Crepidula atrasolea
Leishmania major
Leishmania braziliensis
Trypanosoma cruzi
Trypanosoma brucei brucei
IId
Protists
Adineta steineri
Adineta ricciae
Didymodactylos carnosus
Rotaria magnacalcarata
Rotaria magnacalcarata
Rotaria sordida
Rotifers
Outgroup
Other SAM-dependent MTs
Sponge SMT
Animal sequences
Viridisplantae SMT
Fungal SMT
Protist SMT
Contaminations

Supplementary Figure 22 | Most C-24 sterol methyltransferase (C_{24}-SMT) homologues identified by BLAST within mollusks, chordata and nematode phyla were plant, protist or fungal contaminations, or belonged to the C_4-SMT, an SMT specific to nematodes. Maximum likelihood amino acid tree of SMTs, with other SAM-dependent methyltransferases used as outgroups. Bootstrap values ≥90% are marked with a grey circle. The bootstrap value and branch support value are indicated in brackets for collapsed groups. Animal sequences identified as contamination are labelled in grey. The tree was rooted at midpoint in iTOL. Ubiquinone biosynthesis O-methyltransferase (COQ), phosphoethanolamine N-methyltransferase (PEAMT), tocopherol O-methyltransferase (TMT), C-4 sterol methyltransferase (C_4-SMT).

Supplementary Table 1 | List of sterols detected by MALDI-2-MSI in *Olavius algarvensis*.

Sterol	**Sum formula**	**Molecular weight M** (calc)	**$[M\text{-}H_2O+H]^+$** (calc)	**$[M\text{-}H_2O+H]^+$** (exp)	**Mass error** (ppm)
cholesterol	$C_{27}H_{46}O$	386.355	369.352	369.345	19
sitosterol	$C_{29}H_{50}O$	414.386	397.383	397.376	18
stigmasterol	$C_{29}H_{48}O$	412.371	395.368	395.364	10

Supplementary Table 2 | List of the enzymes involved in sterol biosynthetic pathway in eukaryotic model organisms.

Enzymatic reaction	E.C number	Animal	Plant	Fungi
Squalene monooxygenation	1.14.14.17	SQE	SQE	ERG1
Oxydosqualene cyclization	5.4.99.7 and 5.4.99.8	LAS	CAS	ERG7
C-14 demethylation	1.14.14.154	CYP51	CYP51G1	ERG11
C-14 reduction	1.3.1.70	LBR	FK	ERG24
C-4 demethylation	1.14.18.9 /10 /11	MSMO1	SMO	ERG25
	1.1.1.170 and 1.1.1.418	NSDHL	3β-HSD	ERG26
	1.1.1.270	HSD17B7	?	ERG27
Δ7-Δ8 isomerization	5.-.-.- and 5.3.3.5	EBP	HYD1	ERG2
C-5 desaturation	1.14.19.20 and 1.14.21.6	SC5DL	DWF7	ERG3
Δ7 reduction	1.3.1.21	DHCR7	DWF5	n.d.
Δ24 reduction	1.3.1.71/72 and 1.3.1.M20	DHCR24	DIM	ERG4
C-22 desaturation	1.14.19.41	n.d.	CYP710A	ERG5
C-24 and C-28 methylation	2.1.1.41 and 2.1.1.143	n.d.	SMT	ERG6
Cyclopropylsterol isomerization	5.5.1.9	n.d.	CPI	n.d.

Supplementary Table 3 | Detection of enzymes involved in sterol biosynthesis in the draft genome of *Olavius algarvensis*.

Enzyme	Target	Contig	Status	Reasons	Matches	Mismatch	ID	Coverage	Score	# of exons
SQE	4410_host_Oalg_flye-2.8	contig_6471	incomplete	missing stopcodon + missmatch	515	3	99.4	100	0.988	9
LAS	4410_host_Oalg_flye-2.8	contig_13849	auto	-	756	0	100	100	1	20
CYP51	4410_host_Oalg_flye-2.8	contig_37932	incomplete	mismatches	504	2	99.6	100	0.992	11
CYP51	4410_host_Oalg_flye-2.8	contig_37932	incomplete	mismatches	319	2	99.4	100	0.988	6
LBR	4410_host_Oalg_flye-2.8	contig_20025	partial 1-21 (#1/2)	-	21	0	100	3.6	0.036	1
LBR	4410_host_Oalg_flye-2.8	contig_42201	partial 22-583 (#2/2)	-	555	7	98.8	100	0.94	10
MSMO1	4410_host_Oalg_flye-2.8	contig_24678	incomplete	gap to querystart (7-306)	300	0	NA	NA	0.98	6
NSDHL	4410_host_Oalg_flye-2.8	contig_27038	auto	-	346	0	100	100	1	7
HSD17B7	4410_host_Oalg_flye-2.8	contig_21098	partial 1-27 (#1/2)	-	27	0	NA	NA	0.079	1
HSD17B7	4410_host_Oalg_flye-2.8	contig_21097	partial 18-343 (#2/2)	mismatches + missing stopcodon	312	4	98.7	100	0.898	9
EBP	4410_host_Oalg_flye-2.8	contig_10005	auto	-	230	0	100	100	1	3
SC5DL	4410_host_Oalg_flye-2.8	contig_6195	incomplete	missing stopcodon	282	0	100	100	1	3
DHCR7	4410_host_Oalg_flye-2.8	Contig_8717	incomplete	missing stopcodon + missmatch	482	1	99.8	100	0.996	3
DHCR24	4410_host_Oalg_flye-2.8	scaffold_4022	incomplete	missing stopcodon + missmatch	501	2	99.6	100	0.992	8
SMT	4410_host_Oalg_flye-2.8	contig_41985	incomplete	missing stopcodon	165	0	100	100	1	4

Supplementary Table 4 | Detection of enzymes involved in sterol biosynthesis in the transcriptome of *Olavius algarvensis*.

Enzyme_ID	Contig	Querry	ID (%)	length	evalue	bitscore	assembly
ERG7	TRINITY_DN47299_c3_g1_i19	sp|Q8BLN5|ERG7_MOUSE	61.165	721	0	894	OalgA5SA
ERG6	TRINITY_DN46293_c3_g7_i1	sp|Q9LM02|SMT1_ARATH	49.158	297	8.50E-100	297	OalgA5SA
ERG11	TRINITY_DN47328_c5_g2_i2	sp|Q1JPY5|CYP51_DANRE	69.892	465	0	672	OalgA5SA
ERG1	TRINITY_DN49356_c3_g8_i1	sp|Q14534|ERG1_HUMAN	59.346	428	0	530	OalgA5SA
ERG26	TRINITY_DN40078_c3_g2_i1	sp|Q3ZBE9|NSDHL_BOVIN	60.117	341	1.02E-155	434	OalgB8SA
ERG27	TRINITY_DN48078_c2_g1_i1	sp|Q62904|DHB7_RAT	50	268	2.16E-83	251	OalgA5SA
ERG24	TRINITY_DN29949_c0_g1_i1	sp|Q14739|LBR_HUMAN	49.745	392	6.70E-137	397	OalgB8SA
ERG25	TRINITY_DN35202_c6_g4_i2	sp|Q5ZLL6|MSMO1_CHICK	64.789	284	6.74E-133	375	OalgA8SA
partial_ERG3	TRINITY_DN35917_c0_g1_i2	sp|O75845|SC5D_HUMAN	63.592	206	6.76E-101	301	OalgB5SA
ERG2	TRINITY_DN18361_c0_g1_i2	sp|P70245|EBP_MOUSE	45.249	221	3.50E-72	216	verC3
DHCR7a	TRINITY_DN28908_c0_g1_i1	sp|Q9LDU6|ST7R_ARATH	48.921	417	7.72E-137	394	4731
DHCR24_4731_Verc3_consensus							
partial_DHCR24	TRINITY_DN23155_c0_g1_i1	sp|Q5BQE6|DHC24_RAT	63.725	408	0	574	4731
partial_DHCR24	TRINITY_DN35798_c0_g2_i2	sp|Q5BQE6|DHC24_RAT	63.006	346	5.28E-175	488	verC3

Supplementary Table 5 | Detection of enzymes involved in sterol biosynthesis in the proteome of *Olavius algarvensis*. FDR = False discovery rate, #PSMs = number of peptide spectral matches, #PUPs = number of protein unique peptides.

Protein acession	Description	Found in proteome (filtered for 5% FDR)	Found in # of samples (out of 25)	q-value	#PSMs	#of PUP
ERG1_Host_330784_c8_seq1_40	squalene monooxygenase homologue	No	-	-	-	-
ERG2_Host_282622_c0_seq2_5	sterol C-8 isomerase homologue	Yes	4	0.008	4	0
ERG6_Host_316125_c3_seq1_6	sterol methyltransferase homologue	Yes	25	0	70	4
ERG7_Host_333294_c4_seq2_44	lanosterol synthase homologue	Yes	3	0	4	2
ERG11a_Host_334930_c0_seq4_30	sterol C-14 demethylase homologue	Yes	25	0	50	1
ERG11b_Host_334930_c0_seq1_24	sterol C-14 demethylase homologue	Yes	12	0	16	0
ERG24_Host_331074_c0_seq1_34	sterol C-14 reductase homologue	Yes	25	0	123	5
ERG25_Host_335885_c4_seq2_8	methylsterol monooxygenase homologue	No	-	-	-	-
ERG26a_Host_330893_c3_seq7_9	Sterol-4-alpha-carboxylate 3-dehydrogenase	Yes	17	0	25	1
ERG27_Host_329156_c0_seq5_38	3-keto reductase homologue	No	-	-	-	-
ERG3_Host_326988_c0_seq1_35	sterol C-5 desaturase homologue	No	-	-	-	-
DHCR24_4731_Verc3_concensus	sterol C-24 reductase homologue	No	-	-	-	-
DHCR7a_4731_TRINITY_DN28908_c0_g1_i1	sterol C-7 reductase homologue	No	-	-	-	-

Supplementary Table 6 | The sterol profiles of all investigated *Olavius* and *Inanidrilus* species was dominated by sitosterol.

Species	Sampling location	Main sterol	other sterols	C_{24}-SMT
Olavius algarvensis	Sant'Andrea (Elba, Italy)	sitosterol	cholestrol	yes
Olavius ilvae	Sant'Andrea (Elba, Italy)	sitosterol	cholestrol	yes
Olavius algarvensis	Magaluf (Mallorca, Spain)	sitosterol	cholestrol	yes
Olavius longissimus	Carrie bow Cay (Belize)	sitosterol	cholestrol	yes
Olavius tantulus	Twin Cayes (Belize)	sitosterol	cholestrol	yes
Inanidrilus mojicae	Twin Cayes (Belize)	sitosterol	cholestrol	unknown
Inanidrilus leukodermatus	Carrie bow Cay (Belize)	sitosterol	cholestrol	yes
Olavius sp.	Okinawa (Japan)	sitosterol	cholestrol	yes

Supplementary Table 7 | C_{24}-SMT homologues were identified in the transcriptomes of all *Olavius* and *Inandrilus* species analyzed in this study

Species	Collection site	C_{24}-SMT	Target_ID	Type
Inanidrilus leukodermatus	Harrington Sound (Bermuda)	yes	TRINITY_DN9622	transcript
Inanidrilus sp. FANTCC3	Curlew Cay (Belize)	yes	TRINITY_DN8118	transcript
Inanidrilus sp. NYSP	Carrie Bow Caye (Belize)	yes	TRINITY_DN8686	transcript
Inanidrilus sp. ULE	Curlew Cay (Belize)	yes	TRINITY_DN41110	transcript
Olavius clavatus	Lizard Island (Australia)	yes	g641.t1	gene
Olavius finitimus	Twin Cayes (Belize)	yes	TRINITY_DN10503	transcript
Olavius ilvae	Sant'Andrea (Elba, Italy)	yes	TRINITY_DN18930	transcript and gene
Olavius imperfectus	Twin Cayes (Belize)	yes	TRINITY_DN8834	transcript
Olavius tantalus	Twin Cayes (Belize)	yes	TRINITY_DN12053	transcript

Supplementary Table 8 | C_{24}-SMT homologues are widely spread in annelids. They were found in the transcriptomes of 9 *Olavius* and *Inanidrilus* species, in three deep-sea gutless tubeworm species and 17 gut-bearing annelid species from marine, limnic and terrestrial environments belonging to six different clades. Methylated sterols (C_{28} and C_{29}) often account for an important part of the sterol profile of annelids. References: 1 **(Voogt, 1973b)**, 2 **(Voogt, 1973c)**, 3 (Marsh et al., 1990) , 4 **(McLaughlin, 1971b)**, 5 (Petersen & Holmstrup, 2000), 6 (Hasan et al., 2012), 7 (Zipser et al., 1998), 8 (Naya & Kotake, 1967), 9 (Cerbulis & Wight Taylor, 1969), 10 (Albro et al., 1993), 11 (Mita et al., 2006), 12 (Guan et al., 2021), 13 (Kobayashi et al., 1973), 14 (Phleger et al., 2005), 15 (Rieley et al., 1996).
→ See attached excel file

Supplementary Table 9 | C_{24}-SMT homologues are also present in sponges, rotifers and likely in mollusks.
→ See attached excel file

Supplementary Table 10 | Solvent gradient for high-resolution LC-MS/MS with a C30 column used to identify sterols.

%B	Time (min)
0	-2 (pre-run equilibration)
0	2
16	5.5
45	9
52	12
58	14
66	16
70	18
75	22
97	25
97	32.5
15	33
0	34.4
0	36

Buffer A (60/40 ACN/H_2O, 10 mM ammonium formate, 0.1% FA) and Buffer B (90/10 IPA/ACN, 10 mM ammonium formate, 0.1% FA) were used at a flow rate of 350 µl min^{-1}

Supplementary Table 11 | MS settings of the Q Exactive Plus Orbitrap (Thermo Fisher Scientific) equipped with a HESI probe and a Vanquish Horizon UHPLC System (Thermo Fisher Scientific).

MS^1	**C30 settings**	**C18 settings**
Resolution	70,000	70,000
AGC target	5e5	3e6
Max IT [ms]	65	200
Scan range [*m/z*]	150–1500	100–1000
MS^2	**DDA**	**DIA**
Resolution	35,000	35,000
AGC target	1e6	2e5
Max IT [ms]	75	auto
Loop count	8	1
Dynamic exclusion [sec.]	30	NA
Isolation windows (pos.) [Da]	1	0.4
Isolation windows (neg.) [Da]	1	NA
NCE	30	30

Supplementary Table 12 | List of the enzymes isolated from model organisms used as query to assess the ability of gutless annelids to synthesize sterols.

Enzyme_name	animal	plant	fungi
SQE/ERG1	Q14534	Q9SM02	Q92206
LAS/CAS/ERG7	P48449	P38605	P38604
CYP51/ERG11	Q16850	Q9SAA9	P10614
LBR/FK/ERG24	O76062 Q14739	P32462	Q9LDR4
MSMO1/SMO/ERG25	Q15800	Q8L7W5 Q1EC69 Q9ZW22 Q8VWZ8 F4JLZ6	O59933
NSDHL/3β-HSD/ERG26	Q15738	A9X4U2 Q67ZE1 Q9FX01	P53199
HSD17B7/?/ERG27	P56937	-	Q12452
EBP/HYD1/ERG2	Q15125	O48962	P32352
SC5DL/DWF7/ERG3	O75845	Q39208 Q9M883	P32353
DHCR7/DWF5/-	Q9UBM7	Q9LDU6	-
DHCR24/DIM/ERG4	Q15392	Q39085	P25340
-/CYP710A/ERG5	-	O64697 O64698 Q9ZV28 Q9ZV29	P54781
-/SMT/ERG6	-	Q9LM02 Q39227 Q94JS4	P25087
-/CPI/-	-	Q9M643	-

Supplementary Table 13 | Details of the sequences, plasmid, and *E. coli* cells used for the heterologous gene expression experiments.

Gene Name	Sequence	Length	Restriction Sites to Keep	Cloning Vector	Comment	Expression host	ID
AraTh_Q9LM02	MDLASNLGGKIDKSDVLTAVEKYEQYHVF HGGNEEERKANYTDMVNKYYDLATSFYE YGWGESFHFAQRWKGESLRESIKRHEHF LALQLGIPGQKVLDVGCGIGGPLREIARFS NSVVTGLNNNEYQITRGKELNRLAGVDKT CNFVKADFMMPFPENSFDAVYAIEATCHA PDAYGCYKEIYRVLKPGQCFAAYEWCMT DAFDPDNAEHQKIGEIEIGDGLPDIRLTTKC LEALKQAGFEVIWEKDLAKDSPVPWYLPL DKNHFSLSSFRLTAVGRFTKNMVKILEYIR LAPQGSQRVSNFLEQAAEGDGGRREIFT PMYFFLARKPE	1023 bp	NheI/XhoI	pET-28a(+) with restriction sites NheI/XhoI	His- Tag at the N-terminal side only	*E. coli* C41(DE3)pLysS	T-3784
OclaLIZ1_g641.t1	MTSVEKPSITEILRPLQAKSPSSVESTADG YLRYFEREQQSKDDKVDEEDLDAEATDR RRQDAVTVTNAYYDLATDFYEYGWGDFH FAVLKPEESREHSFAKHEYFLAMKLGLKA GDTVLDIGCGIGGPARHIASLSEANVIGMN INDYQLSRARILTEKAKLDHLCSFVKADYN HMPYGDGHFDVYAIEATCHSPTLLSVYSE VFRVLKPGGMFAVYEWIMTDKYNPTDPY HKKLKADILEGDGLPDIVTAPQAVVAARQA GFEVLESRDRALEPGLPWNVLQARWTLS DIKITPLGRWATHVMLAVLETVHLAPRGAV KVHRTLCKGADALAAAGVEGIFSPMYLLV LRKPRD	1089 bp	NheI/XhoI	pET-28a(+) with restriction sites NheI/XhoI	His- Tag at the N-terminal side only	*E. coli* Lemo21(DE3)	T-3787
OalgB8SA	MNSIEKPSITGILRPLHGKAAVESTADGYL RYFDSDSPPRDDAADADDSDAEAVERRR KNALAVTNAYYDLATDFYEYGWGEAFHFA VLKPEESREHSFAKHEYFLGMKLGLKAGD TVLDIGCGIGGPARHIASLSEANVIGLNIND YQLSRARILTEKAKLDHLCSFVKADYNHMP YGEGHFDKVYAIEATCHSPSLCSVYSEVF RVLKPGGLFALYEWIMTDTYNPTDPYHKK LKADILEGDGLPDLASVPQVLTAARQAGF EVVESRDRALEPGVPWYTVLQARWTLSDI KITPFGRWATHLMLAVLETVRLAPRGSVK VHRTLCKGADALAAAGAEGIFSPMYLLVL RKPSK		NheI/XhoI	pET-28a(+) with restriction sites NheI/XhoI	His- Tag at the N-terminal side only	*E. coli* Lemo21(DE3)	T-3909

Supplementary Table 14 | List of the different sterol substrates tested with the animal C_{24}-SMTs. *Olavius algarvensis* C_{24}-SMT (Oalg_SMT), *Olavius clavatus* C_{24}-SMT (Oclav_SMT) and *Arabidopsis thaliana* C_{24}-SMT (Atha_SMT1). Green shading indicates that the substrate can be used by the enzyme tested. Orange shading indicates that no methylated product was detected at the end of the incubation between the set of enzyme and the substrate tested.

Substrate	Enzyme			Rationale for testing the substrate
	Oalg_SMT	Oclav_SMT	Atha_SMT1	
Lathosterol				Cholesterol intermediate
7-dehydrocholsterol				Cholesterol intermediate
Desmosterol	1st methylation	1st methylation		Cholesterol intermediate
Cholesterol				Cholesterol intermediate
Zymosterol	1st methylation	1st methylation		Substrate of fungal C_{24}-SMT and cholesterol intermadiate
Fecosterol				*(Ganapathy et al., 2008)*
Eburicol				*Pneumocystis carninii*, substrate for 2nd methylation
Lanosterol				Substrate of fungal C_{24}-SMT
Cycloartenol			1st methylation	Substrate of the first methylation in plants
Campesterol				Potential intermediate of *O. algarvensis* sitosterol biosynthesis
24-methylene-cholesterol	2nd methylation	2nd methylation		Potential intermediate of *O. algarvensis* sitosterol biosynthesis

Supplementary Table 15 | Solvent gradient for high-resolution LC-MS/MS with C18 column.

%B	Time (min)
50	-10 (pre-run equilibration)
50	3
87.5	9
90	15
100	21
100	30
50	32

Solvent A (MiliQ, 0.1% FA) and Solvent B (90:10 ACN:MiliQ, 0.1% FA) were used at a flow rate of 200 µl min^{-1}.

References

Albro, P. W., Corbett, J. T., & Schroeder, J. L. (1993). Endogenous lipids of the earthworm *Lumbricus terrestris*. *Biochemistry and Cell Biology*, *71*(3–4), 220–221. https://doi.org/10.1139/o93-033

Ballantine, J. A., Lavis, A., Roberts, J. C., Morris, R. J., Elsworth, J. F., & Cragg, G. M. L. (1978). Marine sterols—VII. The sterol compositions of oceanic and coastal marine annelida species. *Comparative Biochemistry and Physiology Part B: Comparative Biochemistry*, *61*(1), 43–47. https://doi.org/10.1016/0305-0491(78)90211-0

Canuel, E. A., Freeman, K. H., & Wakeham, S. G. (1997). Isotopic compositions of lipid biomarker compounds in estuarine plants and surface sediments. *Limnology and Oceanography*, *42*(7), 1570–1583. https://doi.org/10.4319/lo.1997.42.7.1570

Carvalho, M., Schwudke, D., Sampaio, J. L., Palm, W., Riezman, I., Dey, G., Gupta, G. D., Mayor, S., Riezman, H., Shevchenko, A., Kurzchalia, T. V., & Eaton, S. (2010). Survival strategies of a sterol auxotroph. *Development*, *137*(21), 3675–3685. https://doi.org/10.1242/dev.044560

Cerbulis, J., & Wight Taylor, M. (1969). Neutral lipid and fatty acid composition of earthworms (*Lumbricus terrestris*). *Lipids*, *4*(5), 363–368. https://doi.org/10.1007/BF02531007

Cooper, L., & DeNiro, M. (1989). Stable carbon isotope variability in the seagrass *Posidonia oceanica*: Evidence for light intensity effects. *Marine Ecology Progress Series*, *50*, 225–229. https://doi.org/10.3354/meps050225

Dauby, P. (1989). The stable carbon isotope ratios in benthic food webs of the gulf of Calvi, Corsica. *Continental Shelf Research*, *9*(2), 181–195. https://doi.org/10.1016/0278-4343(89)90091-5

Dubilier, N., Blazejak, A., & Rühland, C. (2006). Symbioses between Bacteria and Gutless Marine Oligochaetes. In J. Overmann (Ed.), *Molecular Basis of Symbiosis* (pp. 251–275). Springer. https://doi.org/10.1007/3-540-28221-1_12

Fry, B., Scalan, R. S., & Parker, P. L. (1983). 13C/12C ratios in marine food webs of the Torres Strait, Queensland. *Marine and Freshwater Research*, *34*(5), 707–715. https://doi.org/10.1071/mf9830707

Ganapathy, K., Jones, C. W., Stephens, C. M., Vatsyayan, R., Marshall, J. A., & Nes, W. D. (2008). Molecular probing of the *Saccharomyces cerevisiae* sterol 24-C methyltransferase reveals multiple amino acid residues involved with C2-transfer activity. *Biochimica et Biophysica Acta (BBA) - Molecular and Cell Biology of Lipids*, *1781*(6), 344–351. https://doi.org/10.1016/j.bbalip.2008.04.015

Guan, H., Birgel, D., Feng, D., Peckmann, J., Liu, L., Liu, L., & Tao, J. (2021). Lipids and their δ13C values reveal carbon assimilation and cycling in the methane-seep tubeworm *Paraescarpia echinospica* from the South China Sea. *Deep Sea Research Part I: Oceanographic Research Papers*, *174*, 103556. https://doi.org/10.1016/j.dsr.2021.103556

Hasan, F., Khar, R. K., Ahmad, F. J., Ahmad, S., Ali, M., Iqbal, Z., & Reza, M. H. (2012). Development and Validation of a Stability-Indicating Method for Determination of Free

Sterols in the Asian Medicinal Leech *Hirudo manillensis*. *Journal of Chromatographic Science*, *50*(8), 673–679. https://doi.org/10.1093/chromsci/bms076

Jennings, S., Reñones, O., Morales-Nin, B., Polunin, N., Moranta, J., & Coll, J. (1997). Spatial variation in the 15N and 13C stable isotope composition of plants, invertebrates and fishes on Mediterranean reefs: Implications for the study of trophic pathways. *Marine Ecology Progress Series*, *146*, 109–116. https://doi.org/10.3354/meps146109

Kobayashi, M., Nishizawa, M., Todo, K., & Mitsuhashi, H. (1973). Marine Sterols. I. Sterols of Annelida, *Pseudopotamilla occelata* MOORE. *Chemical & Pharmaceutical Bulletin*, *21*(2), 323–328. https://doi.org/10.1248/cpb.21.323

Lepoint, G., Dauby, P., & Gobert, S. (2004). Applications of C and N stable isotopes to ecological and environmental studies in seagrass ecosystems. *Marine Pollution Bulletin*, *49*(11), 887–891. https://doi.org/10.1016/j.marpolbul.2004.07.005

Lu, N. C., Newton, C., & Stokstad, E. L. R. (1977). The Requirement of Sterol and Various Sterol Precursors in Free-Living Nematodes. *Nematologica*, *23*(1), 57–61. https://doi.org/10.1163/187529277X00228

Marsh, A. G., Harvey, H. R., Grémare, A., & Tenore, K. R. (1990). Dietary effects on oocyte yolk-composition in *Capitella sp.* I (Annelida: Polychaeta): Fatty acids and sterols. *Marine Biology*, *106*(3), 369–374. https://doi.org/10.1007/BF01344314

McLaughlin, J. (1971a). Biochemical studies on Eisenia foetida (savigny, 1826), the brandling worm—I. Tissue lipids and sterols. *Comparative Biochemistry and Physiology Part B: Comparative Biochemistry*, *38*(1), 147–163. https://doi.org/10.1016/0305-0491(71)90294-X

McLaughlin, J. (1971b). Biochemical studies on Eisenia foetida (savigny, 1826), the brandling worm—I. Tissue lipids and sterols. *Comparative Biochemistry and Physiology Part B: Comparative Biochemistry*, *38*(1), 147–163. https://doi.org/10.1016/0305-0491(71)90294-X

McMillan, C., Parker, P. L., & Fry, B. (1980). 13C12C ratios in seagrasses. *Aquatic Botany*, *9*, 237–249. https://doi.org/10.1016/0304-3770(80)90025-X

Meyer, H., Provasoli, L., & Meyer, F. (1979). Lipid biosynthesis in the marine flatworm *Convoluta roscoffensis* and its algal symbiont *Platymonas convoluta*. *Biochimica Et Biophysica Acta*, *573*(3), 464–480. https://doi.org/10.1016/0005-2760(79)90221-2

Mita, M., Deguchi, M., & Sasayama, Y. (2006). Lipid composition of the trophosome in the beard worm, *Oligobrachia mashikoi* (Pogonophora). *Journal of the Marine Biological Association of the United Kingdom*, *86*(2), 283–286. https://doi.org/10.1017/S0025315406013130

Naya, Y., & Kotake, M. (1967). [Study of free fatty acids, free sterols, sterolester and glyceride in the earthworm (*Lumbricus spencer*)]. *Bulletin of the Chemical Society of Japan*, *40*(4), 880–884.

Oh, K. H., Haney, J. J., Wang, X., Chuang, C.-F., Richmond, J. E., & Kim, H. (2017). ERG-28 controls BK channel trafficking in the ER to regulate synaptic function and alcohol response in *C. elegans*. *ELife*, *6*, e24733. https://doi.org/10.7554/eLife.24733

Petersen, S. O., & Holmstrup, M. (2000). Temperature effects on lipid composition of the earthworms *Lumbricus rubellus* and *Eisenia nordenskioeldi*. *Soil Biology and Biochemistry*, *32*(11), 1787–1791. https://doi.org/10.1016/S0038-0717(00)00059-6

Phleger, C. F., Nelson, M. M., Groce, A. K., Cary, S. C., Coyne, K. J., & Nichols, P. D. (2005). Lipid composition of deep-sea hydrothermal vent tubeworm *Riftia pachyptila*, crabs *Munidopsis subsquamosa* and *Bythograea thermydron*, mussels *Bathymodiolus sp.* And limpets *Lepetodrilus spp. Comparative Biochemistry and Physiology Part B: Biochemistry and Molecular Biology*, *141*(2), 196–210. https://doi.org/10.1016/j.cbpc.2005.03.001

Pinnegar, J. K., & Polunin, N. V. C. (2000). Contributions of stable-isotope data to elucidating food webs of Mediterranean rocky littoral fishes. *Oecologia*, *122*(3), 399–409. https://doi.org/10.1007/s004420050046

Rieley, G., Dover, C. L. V., Hedrick, D. B., White, D. C., & Eglinton, G. (1996). Lipid characteristics of hydrothermal vent organisms from 9°N, East Pacific Rise. *Oceanographic Literature Review*, *2*(43), 133–134.

Shamsuzzama, Lebedev, R., Trabelcy, B., Langier Goncalves, I., Gerchman, Y., & Sapir, A. (2020). Metabolic Reconfiguration in **C. elegans** Suggests a Pathway for Widespread Sterol Auxotrophy in the Animal Kingdom. *Current Biology*, *30*(15), 3031-3038.e7. https://doi.org/10.1016/j.cub.2020.05.070

Sogin, E. M., Michellod, D., Gruber-Vodicka, H., Bourceau, P., Geier, B., Meier, D. V., Seidel, M., Ahmerkamp, S., Schorn, S., D'Angelo, G., Procaccini, G., Dubilier, N., & Liebeke, M. (2021). Sugars dominate the seagrass rhizosphere. *BioRxiv*, 797522. https://doi.org/10.1101/797522

Thayer, G. W., Parker, P. L., LaCroix, M. W., & Fry, B. (1978). The stable carbon isotope ratio of some components of an eelgrass, *Zostera marina*, bed. *Oecologia*, *35*(1), 1–12. https://doi.org/10.1007/BF00345537

Vives-Peris, V., de Ollas, C., Gómez-Cadenas, A., & Pérez-Clemente, R. M. (2020). Root exudates: From plant to rhizosphere and beyond. *Plant Cell Reports*, *39*(1), 3–17. https://doi.org/10.1007/s00299-019-02447-5

Vizzini, S., Tomasello, A., Maida, G. D., Pirrotta, M., Mazzola, A., & Calvo, S. (2010). Effect of explosive shallow hydrothermal vents on δ13C and growth performance in the seagrass *Posidonia oceanica*. *Journal of Ecology*, *98*(6), 1284–1291. https://doi.org/10.1111/j.1365-2745.2010.01730.x

Voogt, P. A. (1973a). Biosynthesis and Composition of Sterols in Annelida. Ii. Investigations On Some Oligochaetes. *Netherlands Journal of Zoology*, *24*(4), 469–478. https://doi.org/10.1163/002829674X00200

Voogt, P. A. (1973b). Biosynthesis and Composition of Sterols in Annelida. Ii. Investigations On Some Oligochaetes. *Netherlands Journal of Zoology*, *24*(4), 469–478. https://doi.org/10.1163/002829674X00200

Voogt, P. A. (1973c). Biosynthesis and Composition of Sterols in Annelida—I. Investigations On Some Polychaetes. *Netherlands Journal of Zoology*, *24*(1), 22–31. https://doi.org/10.1163/002829674X00138

Wacker, A., & Martin-Creuzburg, D. (2012). Biochemical nutrient requirements of the rotifer *Brachionus calyciflorus*: Co-limitation by sterols and amino acids. *Functional Ecology*, *26*(5), 1135–1143. https://doi.org/10.1111/j.1365-2435.2012.02047.x

Wilber, C. G., & Bayors, W. M. (1947). A comparative study of the lipids in some marine annelids. *The Biological Bulletin*, *93*(2), 99–101. https://doi.org/10.2307/1538280

Zipser, B., Bradford, J. J., & Hollingsworth, R. I. (1998). Cholesterol and its derivatives, are the principal steroids isolated from the leech species *Hirudo medicinalis*. *Comparative Biochemistry and Physiology Part C: Pharmacology, Toxicology and Endocrinology*, *120*(2), 269–282. https://doi.org/10.1016/S0742-8413(98)10005-1